UNIVERSITY OF CALIFORNIA
RIVERSIDE

Microtubule Organization at the Cell Cortex is a Determinant of Cell Shape via Division Plane Maintenance and Directional Cell Expansion in Plants

A Dissertation submitted in partial satisfaction
of the requirements for the degree of

Doctor of Philosophy

in

Plant Biology

by

Marschal Allen Bellinger

March 2020

Dissertation Committee:
Dr. Carolyn Rasmussen, Chairperson
Dr. Jaimie Van Norman
Dr. Meng Chen

The dissertation of Marschal Allen Bellinger is approved by:

_____

_____

_____

Committee Chairperson

University of California, Riverside

ACKNOWLEDGEMENTS

In accordance with graduate program guidelines, parts of Chapter 1, are a reprint of a published article in New Phytologist (https://nph.onlinelibrary.wiley.com/):

Carolyn G Rasmussen, Marschal Allen Bellinger (2018) An overview of plant division-plane orientation. New Phytol 219(2): 505-512 DOI: 10.1111/nph.15183,

Initial Research Evaluation Committee:

Carolyn G. Rasmussen

Jaimie M. Van Norman

Linda Walling

Qualifying Exam Committee:

Jaimie M. Van Norman

Meng Chen

Linda Walling

Julia Bailey-Serres

Dawn Nagel

Jeff Bachant

Dissertation Committee:

Carolyn G. Rasmussen

Jaimie M. Van Norman

Meng Chen

Funding:

Graduate Assistance in Area of National Need Fellowship 2017-2018

NSF 1505848

NSF 1716972

Note from Author:

Thank you everyone who has made this work possible. Special thanks to my partner Hans Kohler, my mom Tammie Crislip, and two of the most amazing undergraduate student researchers, Sukhmani Sidhu and Jeffrey Farrow.

ABSTRACT OF THE DISSERTATION

Microtubule Organization at the Cell Cortex is a Determinant of Cell Shape via Division Plane Maintenance and Directional Cell Expansion in Plants

by

Marschal Allen Bellinger

Doctor of Philosophy, Graduate Program in Plant Biology
University of California, Riverside, March 2020
Dr. Carolyn G. Rasmussen, Chairperson

The proper organization of the microtubules is a major determinant of cell shape. Microtubule-associated proteins have essential roles in cell shape determination by direct microtubule interaction. During interphase, microtubules populate the cell cortex and are organized perpendicular to the primary axis of growth. During mitosis, microtubules form conserved structures that are essential for the normal completion of cell division. The preprophase band and phragmoplast are plant specific mitotic microtubule structures. TANGLED1 is localized to the division site and guides the expanding phragmoplast during the later stages of mitosis. To understand more about the role of division site localized proteins and their interacting partners on cell shape determination I analyzed microtubule dynamics, cell shape, and localization of TUBULIN and TANGLED1. I characterized an array of microtubules at the cell cortex during telophase. These microtubules were distinct from the phragmoplast and organized perpendicular to

the division plane as they interacted with the division site and TANGLED1. The density and organization of microtubules in this array was reduced in *tangled1* cells. In wild type cells, we observed individual microtubule addition to the phragmoplast with a preference for the leading edge, however, this preference was lost in *tangled1* mutant cells. The asymmetric bundling of telophase microtubules at the cell cortex with phragmoplast microtubules altered the direction of phragmoplast expansion. These findings reveal a novel mechanism for phragmoplast guidance by division site localized proteins. KINECTIN was previously identified as a TANGLED1 interacting protein. We used *CRISPR*/CAS9 mutagenesis of the *kinectin* gene region in maize to describe a role for KINECTIN as a potential regulator of microtubule associated proteins in plants. The functional protein domains of KINECTIN were revealed by defects in cell expansion and increased cell shape isotropy in *kinectin-1* but not *kinectin-2* mutants. Microtubule dynamicity and TANGLED1 accumulation in the spindle were significantly different in *kinectin-1* mutant cells. Together, our observations provide additional insight into how proper microtubule organization at the cell cortex determines cell shapes in plants via division plane maintenance and directional cell expansion.

TABLE OF CONTENTS

LIST OF FIGURES

LIST OF TABLES

CHAPTER ONE: Microtubule organization regulates division plane positioning and growth.

ABSTRACT

Division plane positioning and directional cell expansion are the two primary pathways for cell shape regulation in plants (Pietra et al. 2013; Ambrose et al. 2007). Cell division is carefully coordinated in both space and time. Symmetric, proliferative, divisions are essential for growth and account for the majority of plant cell divisions. Asymmetric, formative cell divisions are critical for the development of new cell types. Due to their role in development, asymmetric cell divisions are commonly initiated by transcription factors and signalling pathways that define specific, polarized division plane positions (Facette, Rasmussen, and Van Norman 2019). Here, we discuss how the division site at the cell cortex is established and maintained in plant cells during proliferative divisions with a focus on microtubules and microtubule-associated proteins. We also discuss how microtubule organization at the cell cortex during interphase defines cell shapes and plant growth.

INTRODUCTION

The preprophase band is a critical determinant of cell division plane orientation.

Before a cell divides, several requirements must first be met. The cell must reach a minimum size (R. Jones et al. 2017) and the nucleus migrates toward the center of the cell (Wada 2018). Microtubules at the cell cortex condense to form a band that bisects the nucleus and predicts the future cell division site. Interactions between cell cycle regulators and proteins required for division plane establishment have been identified (Hush et al. 1996; Boruc et al. 2010; Spinner et al. 2013; Costa 2017). Typically, proliferative plant cell division divides a cell into two equal volumes at an angle perpendicular to a cell's long axis (Besson and Dumais 2011). This occurs at positions that minimize the surface area of the new cell wall (Martinez et al. 2018). Division plane establishment defects can be identified by analyzing the shape, position, and orientation of the preprophase band in dividing cells and comparing them to a wild type counterpart.

The preprophase band is a plant-specific microtubule, actin filament, and endomembrane structure that is an important determinant of cell division plane orientation (Rasmussen, Wright, and Müller 2013). Actin filament disrupting drugs or mutants cause preprophase band widening and division plane orientation defects (Mineyuki and Palevitz 1990). Mathematical modeling

followed by in-vivo analysis of preprophase band positions revealed that two division plane orientations, transverse and longitudinal, are energetically favored in proliferative cell divisions (Martinez et al. 2018). Recently, the necessity of the preprophase band for proper division plane establishment has been called into question. It has been reported that plant cell divisions proceed independent of preprophase band formation in meiocytes (Otegui and Staehelin 2004), endosperm (Brown and Lemmon 2011), and some moss cells (Doonan et al. 1987; Kosetsu et al. 2017). Regardless, a number of proteins with essential functions in establishment and maintenance of division plane orientation accumulate at the cell cortex together with the condensing preprophase band (Rasmussen and Bellinger 2018).

Normal preprophase band formation requires a complex of conserved type 2A protein phosphatase subunits (PP2A), plant specific proteins and those similar to centrosomal proteins, called the TON1/TRM/PP2A (TTP) complex (Spinner et al. 2013). Key components of this complex were identified by mutants with short, thick stature called *tonneau* (*ton*) (Camilleri et al. 2002; Azimzadeh et al. 2008) and *fass* (Torres-Ruiz and Jürgens 1994). These mutants are unable to form preprophase bands and have division plane orientation defects (Azimzadeh et al. 2008; Spinner et al. 2010; A. Kirik, Ehrhardt, and Kirik 2012). In addition, they have cell elongation defects due to disorganized cell cortex-localized interphase

microtubule arrays (Camilleri et al. 2002; Azimzadeh et al. 2008). Similarly, the maize *fass* homologs *discordia1* and *alternative discordia1* together are required for preprophase band formation and their proteins localize to the division site until preprophase band disassembly (Wright, Gallagher, and Smith 2009; Spinner et al. 2013). The two highly similar genes *TON1A* and *TON1B* are both required for preprophase band formation and have conserved domains shared by centrosomal proteins and both are TTP components. TON1 colocalizes with interphase and preprophase band microtubules at the cell cortex (Azimzadeh et al. 2008). It has also been reported that TON1 interacts with a number of TON1-recruiting motif (TRM) proteins (Drevensek et al. 2012). Several of these proteins bind microtubules and different TRM proteins also interact with other TTP proteins (Spinner et al. 2013). Specificity of the TTP complex may be controlled by TRM proteins with alternative binding specificity for TTP members or microtubules. It is still unclear exactly what proteins are de-phosphorylated by this complex and how this leads to a proper interphase microtubule array and preprophase band organization at the cell cortex.

Interestingly, in animals (Lorson, Horvitz, and van den Heuvel 2000; Yamashita, Jones, and Fuller 2003) and some plants where cell divisions occur independent of preprophase band formation (Kosetsu et al. 2017), it has been reported that spindle orientation plays an essential role in division plane positioning. These

alternative division plane orientation pathways in plants suggest that the preprophase band plays a critical role in division plane maintenance and the coordination of division plane positioning between adjacent cells. It has been observed that preprophase band position will adjust to avoid four-way junctions between cells (Flanders et al. 1990; Martinez et al. 2018). Additionally, it is currently unclear how or when division site-specific proteins accumulate at the cell cortex in preprophase band-independent plant cell divisions (Kosetsu et al. 2017).

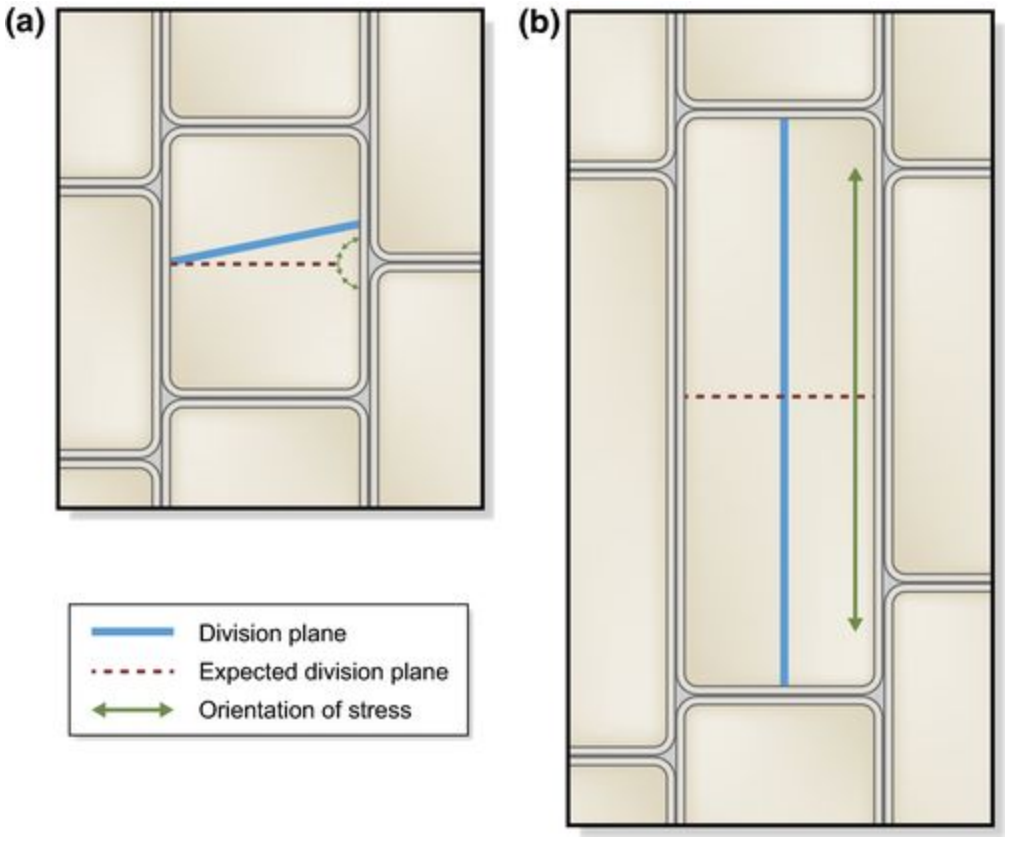

Figure 1.1: Local or tissue-level stress alters division planes to favor positions that would not be predicted by cell shape-based modeling. (a) Local stress (green) at four-way junctions may cause divisions (blue) to shift away from the junction. (b) Division (blue) occurs more frequently (5%) parallel to tissue-level stress (green) and across the longitudinal plane than expected using the 2D Besson–Dumais model (Besson & Dumais, 2011; Louveaux *et al*., 2016).

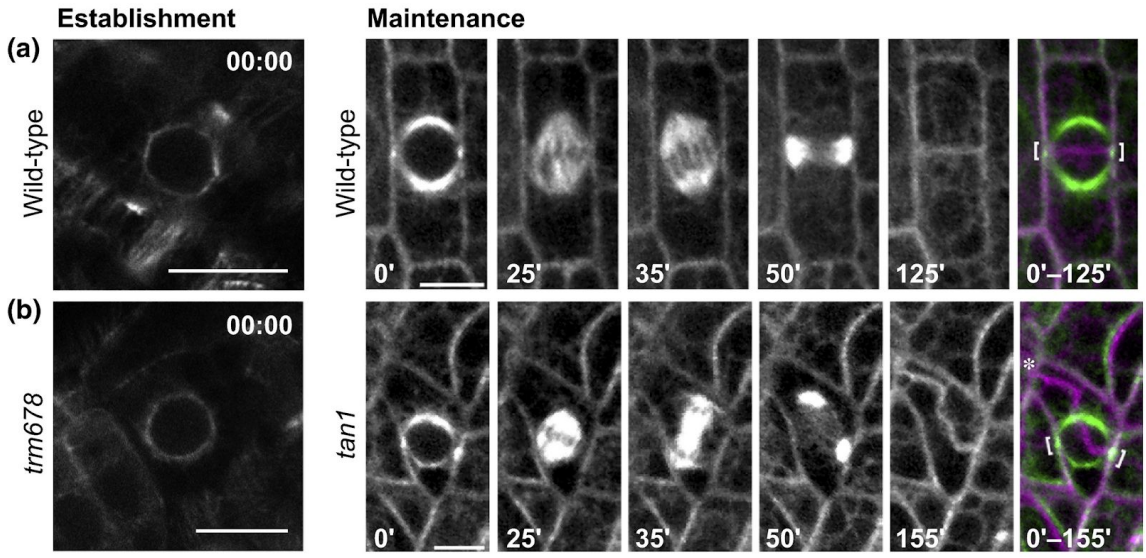

Figure 1.2: Division plane establishment and maintenance. (a) Examples of typical land plant preprophase band (PPB) of wild type Arabidopsis (top left) and mitotic microtubule structures in maize (from prophase with a PPB until the new cell wall is formed, top right). (b) Mutants with defects in division plane establishment lacking a clear PPB (*tonneau1 recruitment motif*, (*trm6,7,8*), bottom left) and maintenance, assessed by time-lapse imaging, when the new cell wall does not return to the location of the PPB (*tangled1 (tan1*) mutant, bottom right). Merged images (far right) show late prophase cells (with PPB in green and indicated with white brackets) and finished cell division (in magenta, asterisk shows misplaced new cell wall). Left panels were modified from (Schaefer *et al*., 2017) and reprinted with permission from the authors and AAAS. Right panels were modified from (Martinez *et al*., 2017a2017b) with permission from the authors. Bars, 10 μm.

The phragmoplast is essential for division plane maintenance.

A number of division site localized proteins accumulate with the preprophase band and remain at the cell cortex following its disassembly (Rasmussen and Bellinger 2018). The role of these proteins is to maintain positional information and to guide the phragmoplast (Walker et al. 2007; Müller, Han, and Smith 2006); (Smertenko et al. 2017), to the correct division site. Division plane maintenance is considered defective when the final division occurs outside of the position specified by the preprophase band (Rasmussen and Bellinger 2018).

The phragmoplast is composed of an antiparallel array of microtubules and actin filaments (McMichael and Bednarek 2013; Livanos and Müller 2019; Smertenko et al. 2018). This structure guides the assembly of the new cell wall as it expands centrifugally outward (Smertenko 2018). Some division site-localized proteins are also found in the phragmoplast midzone (Herrmann et al. 2018; Wu and Bezanilla 2014). However, the initial assembly of the phragmoplast appears to be largely independent of its guidance (Martinez et al. 2017; Herrmann et al. 2018).

The *tangled1* mutant in maize has aberrant cell wall placement and short stature compared to wild-type plants (Smith, Hake, and Sylvester 1996; Cleary and Smith 1998). Live cell imaging revealed that these mutant plants have phragmoplast guidance and mitotic progression defects (Martinez et al. 2017).

TANGLED1 was shown to accumulate at the division site with the maturing preprophase band via a microtubule-dependent mechanism (Rasmussen, Sun, and Smith 2011). Interestingly, it remains at the division site following preprophase band disassembly via a microtubule independent mechanism that requires two related kinesins PHRAGMOPLAST ORIENTING KINESIN1 (POK1) and POK2 (Walker et al. 2007).

The Arabidopsis *tangled1* mutant has only minor division plane orientation and plant growth defects compared to maize (Walker et al. 2007). These defects become exacerbated in the *tan1air9* double mutant (Mir et al. 2018). The AIR9 protein is a microtubule binding protein that localizes to the division site only during preprophase band formation and cell plate insertion (Buschmann et al. 2006). This suggests that the mechanisms of division plane maintenance and phragmoplast guidance are not strictly conserved between monocots and dicots.

Both POK1 and POK2 localize to the division site throughout mitosis and cytokinesis (Müller, Han, and Smith 2006; Herrmann et al. 2018). POK2 was also shown to localize to the phragmoplast midzone (Herrmann et al. 2018). The Arabidopsis *pok1pok2* double mutant has misplaced cell walls and short stature (Müller, Han, and Smith 2006). Apart from a slower expansion speed, there are

no reported defects in the shape or size of the phragmoplast in *pok1pok2* double mutants.

A number of division site localized proteins with roles in division plane maintenance have been shown to interact with POK1 (Müller, Han, and Smith 2006; Schaefer et al. 2017; Rasmussen, Sun, and Smith 2011). Putative Rho-of-plants (ROP) GTPase-activating-proteins (GAP) with pleckstrin homology (PH) domains (PHGAPs) were identified by their interaction with POK1 (Stöckle et al. 2016). These proteins localize to the division site through mitosis. Interestingly, *phgap1phgap2* double mutants express moderate division plane orientation defects and altered POK1 localization at the cell cortex. Together, these reports show that the specific localization of division site proteins can affect division plane maintenance and phragmoplast guidance.

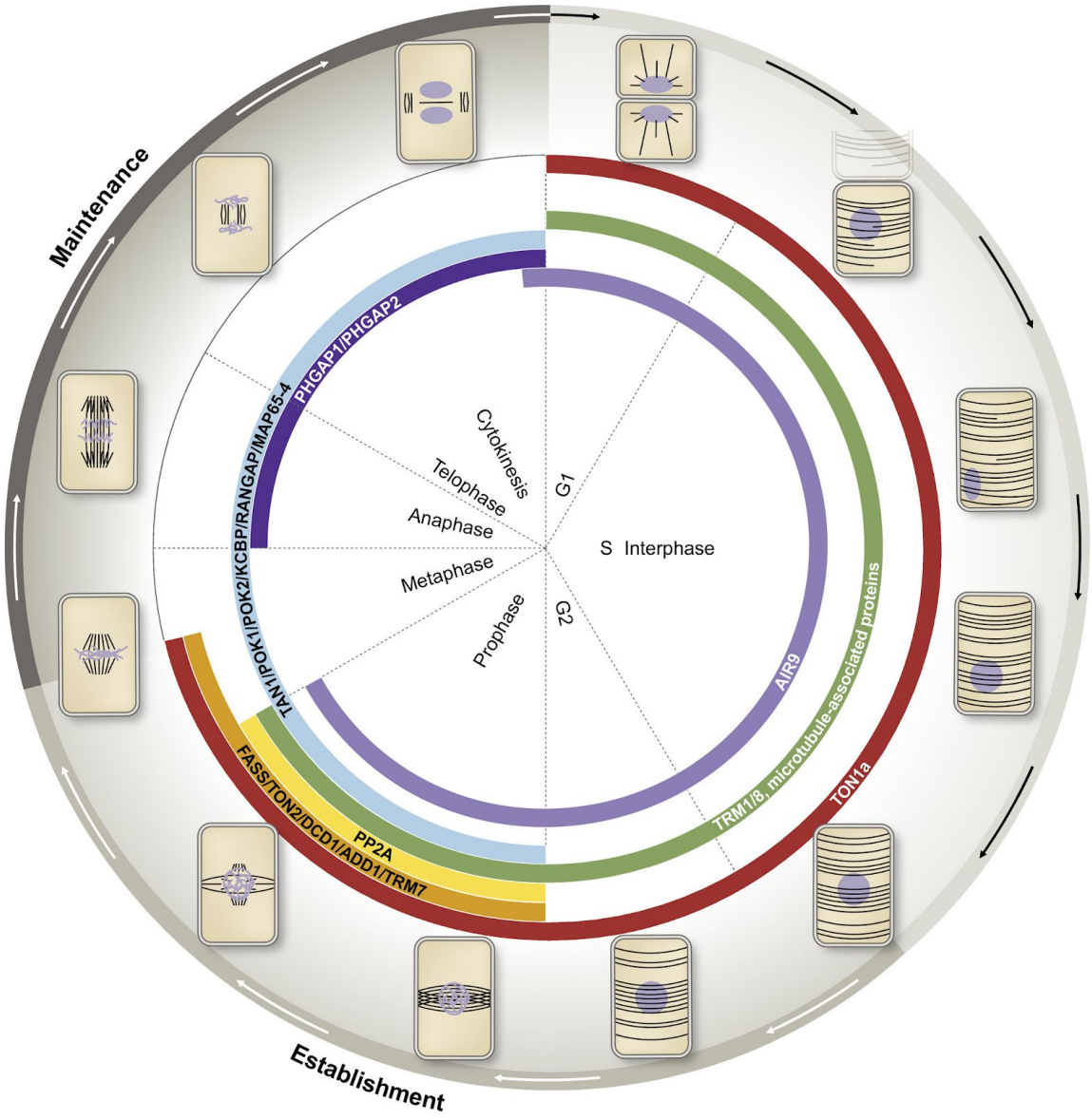
Maintenance
Establishment
Cytokinesis
Telophase
Anaphase
Metaphase
Prophase
G1
S Interphase
G2
PHGAP1/PHGAP2
TAN1/POK1/POK2/KCBP/RANGAP/MAP65-4
AIR9
TRM1/8, microtubule-associated proteins
TON1a
PP2A
FASS/TON2/DCD1/ADD1/TRM7

Figure 1.3: Accumulation of division site localized proteins required for establishment and maintenance of symmetrical plant cell divisions. This schematic representation of the cell cycle indicates key transitions but not the timing of the transitions. The position of cortical microtubule arrays (black) and DNA (violet) of plant cells is shown with phases of the cell cycle. The localization of proteins that promote proper formation of the preprophase band (PPB) are listed under Establishment. TON1a (red) localizes to the interphase microtubule array, then the division site during prophase and part of metaphase (Azimzadeh *et al*., 2008). FASS/TON2/DCD1/ADD1 and TRM7 (orange) localize to the division site from prophase to metaphase (Wright *et al*., 2009; Spinner *et al*., 2013; Schaefer *et al*., 2017). TRM1 and TRM8 (green) localize to the interphase cortical array and the PPB (Drevensek *et al*., 2012; Schaefer *et al*., 2017), similar to many microtubule-binding proteins (Li *et al*., 2015). TAN1, POK1, POK2, KCBP, RAN-GAP and MAP65-4 (blue) localize to the division site from prophase through cytokinesis (Walker *et al*., 2007; Xu *et al*., 2008; Lipka *et al*., 2014; Buschmann *et al*., 2015; Li *et al*., 2017; Martinez *et al*., 2017b). PHGAP1 and PHGAP2 (indigo) localize to the division site from metaphase through cytokinesis (Stöckle *et al*., 2016). AIR9 (violet) localizes to the division site along the violet track, co-localizing with the interphase microtubule array, then co-localizing with the PPB. AIR9 localizes to the division site when the phragmoplast reaches the cell cortex (Buschmann *et al*., 2006).

Microtubule organization at the cell cortex controls cell growth anisotropy during interphase.

Microtubules are intrinsically asymmetric filamentous protein structures made up of alpha and beta-tubulin heterodimers. The microtubule ends with exposed beta-tubulin subunits are said to be the positive-ends. These microtubule ends undergo growth, pause, and shrinkage at faster rates than the minus-ends (Horio and Murata 2014). During interphase, microtubules organize perpendicular to the primary axis of growth (Ambrose et al. 2007; V. Kirik et al. 2007). This specific microtubule organization pattern is critical for the faithful delivery of vesicles and proteins within the cell. Plants with interphase microtubule array organization defects have defects in trichome branching (Buschmann et al. 2009; Abe, Thitamadee, and Hashimoto 2004), root hair or pollen tube elongation (Wang et al. 2007; Zhu et al. 2013; Kang et al. 2017) and overall plant growth (Camilleri et al. 2002; Ambrose et al. 2007).

KINESINS, DYNEINS and MYOSINS are three major classes of motor proteins (Hirokawa et al. 2009). These proteins move cargo along microtubules or actin filaments and can alter the organization of microtubules within a cell. Most KINESIN motor proteins move toward the microtubule plus-end in animal cells, while DYNEIN motor proteins move toward the microtubule minus-end. Intriguingly, plants do not have DYNEIN motor proteins, but instead a gene family

that encodes microtubule minus-end directed KINESIN proteins has been expanded and is thought to fulfill this role in plant cells (Nebenführ and Dixit 2018; Gicking et al. 2018). POK1 and POK2 are examples of this protein family that are specifically expressed during mitosis in plant cells (Müller, Han, and Smith 2006). Recently, it was revealed that the motor domain of POK2 is microtubule plus-end directed (Chugh et al. 2018).

To move cargo along microtubules, motor proteins must form dimers or tetramers (Hirokawa et al. 2009). The motor, neck, stalk, and tail are the fundamental protein domains that define all motor proteins (Nebenführ and Dixit 2018). The motor domain attaches and detaches from microtubules in an ATP-dependent manner. When the motor domain is in an ADP-associated form it is attached to the microtubule (Atherton et al. 2014). The stalk domain is primarily composed of interspersed coiled-coil domains and is important for protein-protein interactions. The speed of motor protein movement is regulated by the length of the neck domain and protein interactions at the stalk domain (Endow, Kull, and Liu 2010). The tail domain is important for cargo sorting and motor domain inhibition (Hackney and Stock 2008; Friedman and Vale 1999).

Sequence identity at the amino acid level is highly conserved among motor proteins in plants (Nebenführ and Dixit 2018). One motor protein regulator that

has been described in the animal literature is KINECTIN (Kumar, Yu, and Sheetz 1995). The KINECTIN protein was found to directly bind KINESIN-1 in vitro (Ong et al. 2000). KINECTIN-like proteins are conserved in plants (Kwon et al. 2018; Chehab, Patharkar, and Cushman 2007; Park et al. 2014).

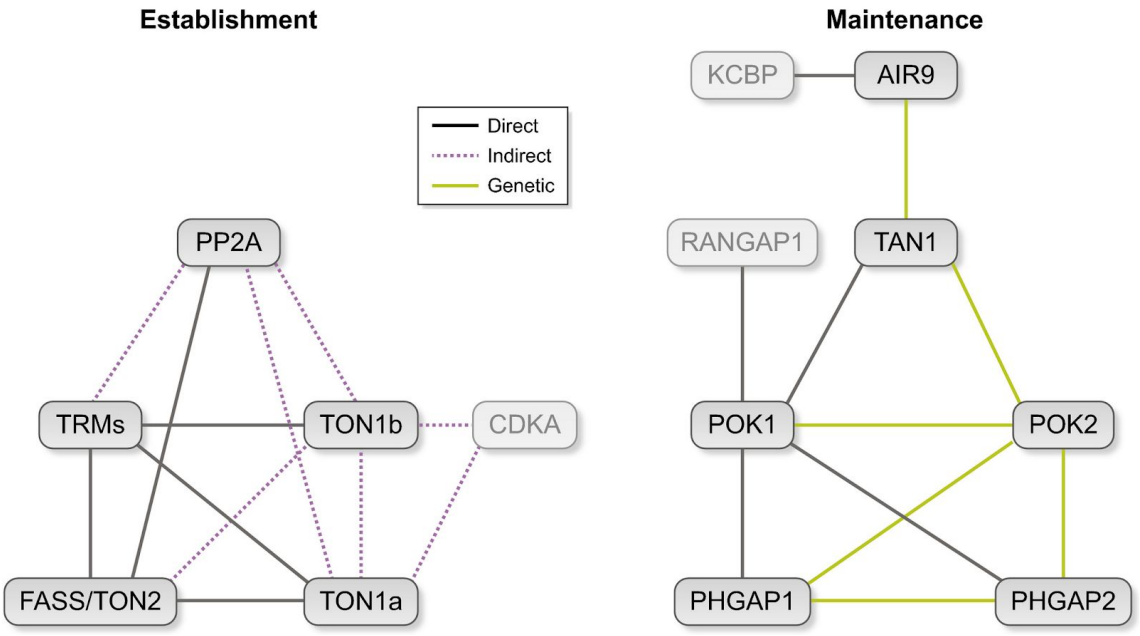

Figure 1.4: A schematic of the currently known division plane establishment and maintenance interactions. Potentially indirect protein–protein interactions identified by mass spectrometry are indicated with dotted magenta lines, direct protein–protein interactions are indicated with black lines, whereas genetic interactions are indicated with green lines. Establishment: the components of the TON1/TRM/PP2A (TTP) complex. TON1a interacts with TON1b (Spinner *et al*., 2013). FASS/TON2 interacts with TON1a, TON1b and PP2A (Spinner *et al*., 2013). TRM1 interacts with TON1a via a region of TRM1 containing conserved domain 2 (Drevensek *et al*., 2012). TON1a interacts with multiple TRMs (2, 3, 7, 11, 14, 19, 20, 21, 22, 25 and 26) (Drevensek *et al*., 2012). TRM19 interacts with TON1, FASS/TON2 and PP2A (Spinner *et al*., 2013). TRM1, TRM3 and TRM29 interact with FASS/TON2, probably via interaction with conserved TRM domain 3 (Spinner *et al*., 2013). CDKA interacts with TON1a (Spinner *et al*., 2013; Costa, 2017) and TON1b (Van Leene *et al*., 2007): genetic interactions suggest that speeding up cell cycle progression worsens division plane defects of *ton1a* mutants (Costa, 2017). Maintenance: POK1 interacts with TAN1 (Müller *et al*., 2006; Walker *et al*., 2007; Rasmussen *et al*., 2011b), RAN-GAP (Xu *et al*., 2008) and PHGAP1 and 2 (Stöckle *et al*., 2016). *tan1 air9* double mutants have a synthetic division plane orientation defect suggesting genetic interaction (Mir *et al*., 2018). AIR9 physically interacts with KCBP (Buschmann *et al*., 2015). CDKA, KCBP and RANGAP1 are labeled in gray to reflect that specific roles in division plane establishment or maintenance are still unclear. This model reflects our current understanding of division plane establishment and maintenance, but there are likely as-yet-unidentified proteins and interactions between them.

Research Outline

In this thesis work I aim to understand the influence of microtubule organization on cell shape via division plane maintenance and anisotropic organization of microtubules at the cell cortex through the function of TANGLED1 and KINECTIN respectively. In chapter 2, I describe how microtubules at the cell cortex organize toward the division plane and interact with the phragmoplast in a TANGLED1-dependant manner to guide the phragmoplast. In chapter 3, I describe a novel role for KINECTIN, a TANGLED1 interacting protein, as a regulator microtubule organization and cell shape. In Chapter 4, I summarize this work and propose future experiments.

REFERENCES

Abe, Tatsuya, Siripong Thitamadee, and Takashi Hashimoto. 2004. “Microtubule Defects and Cell Morphogenesis in the lefty1lefty2 Tubulin Mutant of Arabidopsis Thaliana.” *Plant & Cell Physiology* 45 (2): 211–20.

Ambrose, J. Christian, Tsubasa Shoji, Amanda M. Kotzer, Jamie A. Pighin, and Geoffrey O. Wasteneys. 2007. “The Arabidopsis CLASP Gene Encodes a Microtubule-Associated Protein Involved in Cell Expansion and Division.” *The Plant Cell* 19 (9): 2763–75.

Atherton, Joseph, Irene Farabella, I-Mei Yu, Steven S. Rosenfeld, Anne Houdusse, Maya Topf, and Carolyn A. Moores. 2014. “Conserved Mechanisms of Microtubule-Stimulated ADP Release, ATP Binding, and Force Generation in Transport Kinesins.” *eLife* 3 (September): e03680.

Azimzadeh, Juliette, Philippe Nacry, Anna Christodoulidou, Stéphanie Drevensek, Christine Camilleri, Nardjis Amiour, François Parcy, Martine Pastuglia, and David Bouchez. 2008. “Arabidopsis TONNEAU1 Proteins Are Essential for Preprophase Band Formation and Interact with Centrin.” *The Plant Cell* 20 (8): 2146–59.

Besson, Sébastien, and Jacques Dumais. 2011. “Universal Rule for the Symmetric Division of Plant Cells.” *Proceedings of the National Academy of Sciences of the United States of America* 108 (15): 6294–99.

Boruc, Joanna, Evelien Mylle, Maria Duda, Rebecca De Clercq, Stephane Rombauts, Danny Geelen, Pierre Hilson, Dirk Inzé, Daniel Van Damme, and Eugenia Russinova. 2010. “Systematic Localization of the Arabidopsis Core Cell Cycle Proteins Reveals Novel Cell Division Complexes.” *Plant Physiology* 152 (2): 553–65.

Brown, Roy C., and Betty E. Lemmon. 2011. “Dividing without Centrioles: Innovative Plant Microtubule Organizing Centres Organize Mitotic Spindles in Bryophytes, the Earliest Extant Lineages of Land Plants.” *AoB Plants* 2011 (November): lr028.

Buschmann, Henrik, Jordi Chan, Luis Sanchez-Pulido, Miguel A. Andrade-Navarro, John H. Doonan, and Clive W. Lloyd. 2006. “Microtubule-Associated AIR9 Recognizes the Cortical Division Site at Preprophase and Cell-Plate Insertion.” *Current Biology: CB* 16 (19): 1938–43.

Buschmann, Henrik, Monika Hauptmann, Dierk Niessing, Clive W. Lloyd, and Anton R. Schäffner. 2009. “Helical Growth of the Arabidopsis Mutant tortifolia2 Does Not Depend on Cell Division Patterns but Involves Handed Twisting of Isolated Cells.” *The Plant Cell* 21 (7): 2090–2106.

Camilleri, Christine, Juliette Azimzadeh, Martine Pastuglia, Catherine Bellini, Olivier Grandjean, and David Bouchez. 2002. “The Arabidopsis TONNEAU2 Gene Encodes a Putative Novel Protein Phosphatase 2A Regulatory Subunit Essential for the Control of the Cortical Cytoskeleton.” *The Plant Cell* 14 (4): 833–45.

Chehab, E. Wassim, O. Rahul Patharkar, and John C. Cushman. 2007. “Isolation and Characterization of a Novel v-SNARE Family Protein That Interacts with a Calcium-Dependent Protein Kinase from the Common Ice Plant, Mesembryanthemum Crystallinum.” *Planta* 225 (4): 783–99.

Chugh, Mayank, Maja Reißner, Michael Bugiel, Elisabeth Lipka, Arvid Herrmann, Basudev Roy, Sabine Müller, and Erik Schäffer. 2018. “Phragmoplast Orienting Kinesin 2 Is a Weak Motor Switching between Processive and Diffusive Modes.” *Biophysical Journal* 115 (2): 375–85.

Cleary, A. L., and L. G. Smith. 1998. “The Tangled1 Gene Is Required for Spatial Control of Cytoskeletal Arrays Associated with Cell Division during Maize Leaf Development.” *The Plant Cell* 10 (11): 1875–88.

Costa, Silvia. 2017. “Are Division Plane Determination and Cell-Cycle Progression Coordinated?” *The New Phytologist* 213 (1): 16–21.

Doonan, John H., David J. Cove, Fiona M. K. Corke, and Clive W. Lloyd. 1987. “Pre-Prophase Band of Microtubules, Absent from Tip-Growing Moss Filaments, Arises in Leafy Shoots during Transition to Intercalary Growth.” *Cell Motility and the Cytoskeleton* 7 (2): 138–53.

Drevensek, Stéphanie, Magali Goussot, Yann Duroc, Anna Christodoulidou, Sylvie Steyaert, Estelle Schaefer, Evelyne Duvernois, et al. 2012. “The Arabidopsis TRM1-TON1 Interaction Reveals a Recruitment Network Common to Plant Cortical Microtubule Arrays and Eukaryotic Centrosomes.” *The Plant Cell* 24 (1): 178–91.

Endow, Sharyn A., F. Jon Kull, and Honglei Liu. 2010. “Kinesins at a Glance.” *Journal of Cell Science* 123 (Pt 20): 3420–24.

Facette, Michelle R., Carolyn G. Rasmussen, and Jaimie M. Van Norman. 2019. “A Plane Choice: Coordinating Timing and Orientation of Cell Division during Plant Development.” *Current Opinion in Plant Biology* 47 (February): 47–55.

Flanders, D. J., D. J. Rawlins, P. J. Shaw, and C. W. Lloyd. 1990. “Nucleus-Associated Microtubules Help Determine the Division Plane of Plant Epidermal Cells: Avoidance of Four-Way Junctions and the Role of Cell Geometry.” *The Journal of Cell Biology* 110 (4): 1111–22.

Friedman, D. S., and R. D. Vale. 1999. “Single-Molecule Analysis of Kinesin Motility Reveals Regulation by the Cargo-Binding Tail Domain.” *Nature Cell Biology* 1 (5): 293–97.

Gicking, Allison M., Kyle W. Swentowsky, R. Kelly Dawe, and Weihong Qiu. 2018. “Functional Diversification of the Kinesin-14 Family in Land Plants.” *FEBS Letters* 592 (12): 1918–28.

Hackney, David D., and Maryanne F. Stock. 2008. “Kinesin Tail Domains and Mg2+ Directly Inhibit Release of ADP from Head Domains in the Absence of Microtubules.” *Biochemistry* 47 (29): 7770–78.

Herrmann, Arvid, Pantelis Livanos, Elisabeth Lipka, Astrid Gadeyne, Marie-Theres Hauser, Daniël Van Damme, and Sabine Müller. 2018. “Dual Localized Kinesin-12 POK2 Plays Multiple Roles during Cell Division and Interacts with MAP65-3.” *EMBO Reports*, July. https://doi.org/10.15252/embr.201846085.

Hirokawa, Nobutaka, Yasuko Noda, Yosuke Tanaka, and Shinsuke Niwa. 2009. “Kinesin Superfamily Motor Proteins and Intracellular Transport.” *Nature Reviews. Molecular Cell Biology* 10 (10): 682–96.

Horio, Tetsuya, and Takashi Murata. 2014. “The Role of Dynamic Instability in Microtubule Organization.” *Frontiers in Plant Science* 5 (October): 511.

Hush, J., L. Wu, P. C. John, L. H. Hepler, and P. K. Hepler. 1996. “Plant Mitosis Promoting Factor Disassembles the Microtubule Preprophase Band and Accelerates Prophase Progression in Tradescantia.” *Cell Biology International* 20 (4): 275–87.

Kang, Erfang, Mingzhi Zheng, Yan Zhang, Ming Yuan, Shaul Yalovsky, Lei Zhu, and Ying Fu. 2017. “The Microtubule-Associated Protein MAP18 Affects ROP2 GTPase Activity during Root Hair Growth.” *Plant Physiology* 174 (1): 202–22.

Kirik, Angela, David W. Ehrhardt, and Viktor Kirik. 2012. “TONNEAU2/FASS Regulates the Geometry of Microtubule Nucleation and Cortical Array Organization in Interphase Arabidopsis Cells.” *The Plant Cell* 24 (3): 1158–70.

Kirik, Viktor, Ullrich Herrmann, Chaithanyarani Parupalli, John C. Sedbrook, David W. Ehrhardt, and Martin Hülskamp. 2007. “CLASP Localizes in Two Discrete Patterns on Cortical Microtubules and Is Required for Cell Morphogenesis and Cell Division in Arabidopsis.” *Journal of Cell Science* 120 (Pt 24): 4416–25.

Kosetsu, Ken, Takashi Murata, Moé Yamada, Momoko Nishina, Joanna Boruc, Mitsuyasu Hasebe, Daniël Van Damme, and Gohta Goshima. 2017. “Cytoplasmic MTOCs Control Spindle Orientation for Asymmetric Cell Division in Plants.”

Proceedings of the National Academy of Sciences of the United States of America 114 (42): E8847–54.

Kumar, J., H. Yu, and M. P. Sheetz. 1995. “Kinectin, an Essential Anchor for Kinesin-Driven Vesicle Motility.” *Science* 267 (5205): 1834–37.

Kwon, Yun, Jinbo Shen, Myoung Hui Lee, Kyoung Rok Geem, Liwen Jiang, and Inhwan Hwang. 2018. “AtCAP2 Is Crucial for Lytic Vacuole Biogenesis during Germination by Positively Regulating Vacuolar Protein Trafficking.” *Proceedings of the National Academy of Sciences of the United States of America* 115 (7): E1675–83.

Livanos, Pantelis, and Sabine Müller. 2019. “Division Plane Establishment and Cytokinesis.” *Annual Review of Plant Biology*, February. https://doi.org/10.1146/annurev-arplant-050718-100444.

Lorson, M. A., H. R. Horvitz, and S. van den Heuvel. 2000. “LIN-5 Is a Novel Component of the Spindle Apparatus Required for Chromosome Segregation and Cleavage Plane Specification in Caenorhabditis Elegans.” *The Journal of Cell Biology* 148 (1): 73–86.

Martinez, Pablo, Lindy A. Allsman, Kenneth A. Brakke, Christopher Hoyt, Jordan Hayes, Hong Liang, Wesley Neher, et al. 2018. “Predicting Division Planes of Three-Dimensional Cells by Soap-Film Minimization.” *The Plant Cell* 30 (10): 2255–66.

Martinez, Pablo, Anding Luo, Anne Sylvester, and Carolyn G. Rasmussen. 2017. “Proper Division Plane Orientation and Mitotic Progression Together Allow Normal Growth of Maize.” *Proceedings of the National Academy of Sciences of the United States of America* 114 (10): 2759–64.

McMichael, Colleen M., and Sebastian Y. Bednarek. 2013. “Cytoskeletal and Membrane Dynamics during Higher Plant Cytokinesis.” *The New Phytologist* 197 (4): 1039–57.

Mineyuki, Y., and B. A. Palevitz. 1990. “Relationship between Preprophase Band Organization, F-Actin and the Division Site in Allium: Fluorescence and Morphometric Studies on Cytochalasin-Treated Cells.” *Journal of Cell Science* 97 (2): 283–95.

Mir, Ricardo, Victoria H. Morris, Henrik Buschmann, and Carolyn G. Rasmussen. 2018. “Division Plane Orientation Defects Revealed by a Synthetic Double Mutant Phenotype.” *Plant Physiology* 176 (1): 418–31.

Müller, Sabine, Shengcheng Han, and Laurie G. Smith. 2006. “Two Kinesins Are Involved in the Spatial Control of Cytokinesis in Arabidopsis Thaliana.” *Current Biology: CB* 16 (9): 888–94.

Nebenführ, Andreas, and Ram Dixit. 2018. “Kinesins and Myosins: Molecular Motors That Coordinate Cellular Functions in Plants.” *Annual Review of Plant Biology* 69 (April): 329–61.

Ong, L. L., A. P. Lim, C. P. Er, S. A. Kuznetsov, and H. Yu. 2000. “Kinectin-Kinesin Binding Domains and Their Effects on Organelle Motility.” *The Journal of Biological Chemistry* 275 (42): 32854–60.

Otegui, Marisa S., and L. Andrew Staehelin. 2004. “Electron Tomographic Analysis of Post-Meiotic Cytokinesis during Pollen Development in Arabidopsis Thaliana.” *Planta* 218 (4): 501–15.

Park, Guen Tae, Jennifer M. Frost, Jin-Sup Park, Tae Ho Kim, Jong Seob Lee, Sung Aeong Oh, David Twell, Janie Sue Brooks, Robert L. Fischer, and Yeonhee Choi. 2014. “Nucleoporin MOS7/Nup88 Is Required for Mitosis in Gametogenesis and Seed Development in Arabidopsis.” *Proceedings of the National Academy of Sciences of the United States of America* 111 (51): 18393–98.

Pietra, Stefano, Anna Gustavsson, Christian Kiefer, Lothar Kalmbach, Per Hörstedt, Yoshihisa Ikeda, Anna N. Stepanova, Jose M. Alonso, and Markus Grebe. 2013. “Arabidopsis SABRE and CLASP Interact to Stabilize Cell Division Plane Orientation and Planar Polarity.” *Nature Communications* 4: 2779.

Rasmussen, Carolyn G., and Marschal Bellinger. 2018. “An Overview of Plant Division-Plane Orientation.” *The New Phytologist*, April. https://doi.org/10.1111/nph.15183.

Rasmussen, Carolyn G., Brian Sun, and Laurie G. Smith. 2011. “Tangled Localization at the Cortical Division Site of Plant Cells Occurs by Several Mechanisms.” *Journal of Cell Science* 124 (Pt 2): 270–79.

Rasmussen, Carolyn G., Amanda J. Wright, and Sabine Müller. 2013. “The Role of the Cytoskeleton and Associated Proteins in Determination of the Plant Cell Division Plane.” *The Plant Journal: For Cell and Molecular Biology* 75 (2): 258–69.

R. Jones, Angharad, Manuel Forero-Vargas, Simon P. Withers, Richard S. Smith, Jan Traas, Walter Dewitte, and James A. H. Murray. 2017. “Cell-Size Dependent Progression of the Cell Cycle Creates Homeostasis and Flexibility of Plant Cell Size.” *Nature Communications* 8 (1): 15060.

Schaefer, Estelle, Katia Belcram, Magalie Uyttewaal, Yann Duroc, Magali Goussot, David Legland, Elise Laruelle, Marie-Ludivine de Tauzia-Moreau, Martine Pastuglia, and David Bouchez. 2017. “The Preprophase Band of Microtubules Controls the Robustness of Division Orientation in Plants.” *Science* 356 (6334): 186–89.

Smertenko, Andrei. 2018. “Phragmoplast Expansion: The Four-Stroke Engine That Powers Plant Cytokinesis.” *Current Opinion in Plant Biology* 46 (December): 130–37.

Smertenko, Andrei, Farhah Assaad, František Baluška, Magdalena Bezanilla, Henrik Buschmann, Georgia Drakakaki, Marie-Theres Hauser, et al. 2017. “Plant Cytokinesis: Terminology for Structures and Processes.” *Trends in Cell Biology* 27 (12): 885–94.

Smertenko, Andrei, Seanna L. Hewitt, Caitlin N. Jacques, Rafal Kacprzyk, Yan Liu, Matthew J. Marcec, Lindani Moyo, et al. 2018. “Phragmoplast Microtubule Dynamics - a Game of Zones.” *Journal of Cell Science* 131 (2). https://doi.org/10.1242/jcs.203331.

Smith, L. G., S. Hake, and A. W. Sylvester. 1996. “The Tangled-1 Mutation Alters Cell Division Orientations throughout Maize Leaf Development without Altering Leaf Shape.” *Development* 122 (2): 481–89.

Spinner, Lara, Astrid Gadeyne, Katia Belcram, Magali Goussot, Michaël Moison, Yann Duroc, Dominique Eeckhout, et al. 2013. “A Protein Phosphatase 2A Complex Spatially Controls Plant Cell Division.” *Nature Communications* 4: 1863.

Spinner, Lara, Martine Pastuglia, Katia Belcram, Mathieu Pegoraro, Magali Goussot, David Bouchez, and Didier G. Schaefer. 2010. “The Function of TONNEAU1 in Moss Reveals Ancient Mechanisms of Division Plane Specification and Cell Elongation in Land Plants.” *Development* 137 (16): 2733–42.

Stöckle, Dorothee, Arvid Herrmann, Elisabeth Lipka, Theresa Lauster, Richard Gavidia, Steffi Zimmermann, and Sabine Müller. 2016. “Putative RopGAPs Impact Division Plane Selection and Interact with Kinesin-12 POK1.” *Nature Plants* 2 (August): 16120.

Torres-Ruiz, R. A., and G. Jürgens. 1994. “Mutations in the FASS Gene Uncouple Pattern Formation and Morphogenesis in Arabidopsis Development.” *Development* 120 (10): 2967–78.

Wada, Masamitsu. 2018. “Nuclear Movement and Positioning in Plant Cells.” *Seminars in Cell & Developmental Biology* 82 (October): 17–24.

Walker, Keely L., Sabine Müller, Dorianne Moss, David W. Ehrhardt, and Laurie G. Smith. 2007. “Arabidopsis TANGLED Identifies the Division Plane throughout Mitosis and Cytokinesis.” *Current Biology: CB* 17 (21): 1827–36.

Wang, Xia, Lei Zhu, Baoquan Liu, Che Wang, Lifeng Jin, Qian Zhao, and Ming Yuan. 2007. “Arabidopsis MICROTUBULE-ASSOCIATED PROTEIN18 Functions in

Directional Cell Growth by Destabilizing Cortical Microtubules." *The Plant Cell* 19 (3): 877–89.

Wright, Amanda J., Kimberly Gallagher, and Laurie G. Smith. 2009. "discordia1 and Alternative discordia1 Function Redundantly at the Cortical Division Site to Promote Preprophase Band Formation and Orient Division Planes in Maize." *The Plant Cell* 21 (1): 234–47.

Wu, Shu-Zon, and Magdalena Bezanilla. 2014. "Myosin VIII Associates with Microtubule Ends and Together with Actin Plays a Role in Guiding Plant Cell Division." *eLife* 3 (September). https://doi.org/10.7554/eLife.03498.

Yamashita, Yukiko M., D. Leanne Jones, and Margaret T. Fuller. 2003. "Orientation of Asymmetric Stem Cell Division by the APC Tumor Suppressor and Centrosome." *Science* 301 (5639): 1547–50.

Zhu, Lei, Yan Zhang, Erfang Kang, Qiangyi Xu, Miaoying Wang, Yue Rui, Baoquan Liu, Ming Yuan, and Ying Fu. 2013. "MAP18 Regulates the Direction of Pollen Tube Growth in Arabidopsis by Modulating F-Actin Organization." *The Plant Cell* 25 (3): 851–67.

CHAPTER TWO: Cortically localized telophase microtubules contribute to division plane positioning in plant cells

ABSTRACT

Proper cell division plane positioning is critical for normal development in plants and animals. Plants have two unique microtubule structures that are essential for division plane establishment and maintenance, the preprophase band and phragmoplast (Livanos and Müller 2019; Rasmussen and Bellinger 2018). The phragmoplast is a microtubule and microfilament structure that becomes apparent during telophase (Smertenko et al. 2017). In proliferative divisions, the phragmoplast expands outwards from the center of the cell toward a location at the cell cortex called the division site (Smertenko 2018). Proteins that are essential for phragmoplast guidance to the division site have been identified (Rasmussen and Bellinger 2018). However, it is still unknown how phragmoplast guidance is achieved by these proteins. I show that cell cortex-localized microtubules nucleated during the anaphase to telophase transition and distinct are from the phragmoplast. These microtubules were organized by the putative division site and oriented perpendicular to the division plane. I observed that cell cortex-localized telophase microtubules were locally added into the phragmoplast by parallel bundling. I found that the asymmetric accumulation of telophase microtubules at the cell cortex corresponded to alterations in the direction of

phragmoplast expansion. Further, cell cortex localized telophase microtubules were misoriented or absent in the phragmoplast guidance defective *tangled1* maize mutant. These observations suggest that proper phragmoplast guidance is achieved by TANGLED1 via division site specific organization of microtubules at the cell cortex during telophase.

INTRODUCTION

The division site is located at the cell cortex and made apparent during plant cell division by the preprophase band. Proteins with division plane maintenance functions localize to this position at the cell cortex (Rasmussen and Bellinger 2018; Smertenko et al. 2017). The phragmoplast is critical for assembling the cell plate, a cell wall precursor, which divides two daughter cells (Smertenko 2018). The phragmoplast progressively expands toward the division site via new microtubule nucleation from pre-existing microtubules at the leading edge (Murata et al. 2013; Lee and Liu 2013). Phragmoplast dynamics are regulated internally by a number of microtubule-associated proteins, including the mitosis specific kinesin-like protein (NACK/HINKEL/TETRSPORE), the kinases NPK1, RUNKEL and the microtubule crosslinking protein MAP65 (Li et al. 2017; Sasabe and Machida 2012). How the phragmoplast is directed towards the division site is still unknown (Livanos and Müller 2019; Rasmussen and Bellinger 2018).

Several proteins accumulate at the division site with the maturing preprophase band and remain at this location following preprophase band disassembly (Rasmussen and Bellinger 2018). Division site localized proteins, such as TANGLED1, POK1 and POK2 are thought to recruit the phragmoplast to the division site because *tangle1* and *pok1/2* double mutants have defects in phragmoplast guidance (Müller, Han, and Smith 2006; Martinez et al. 2017; Cleary and Smith 1998; Herrmann et al. 2018; Stöckle et al. 2016). These and other division site localized proteins are microtubule or microfilament associated proteins, suggesting that division plane maintenance may be achieved through altered cytoskeleton dynamics (Wu and Bezanilla 2014; Müller, Han, and Smith 2006; Chugh et al. 2018; Martinez et al. 2019).

Microtubules and microtubule nucleating factors such as gamma-tubulin and the gamma-tubulin ring complex have been observed at the cell cortex during telophase in plants (Kong et al. 2010; Liu, Palevitz, and Joshi 1995; Wick 1985). A proposed function for these cortical microtubules is to prepopulate the cell cortex ahead of G1, when microtubules dynamically rearrange following mitosis (Flanders et al 1990). I demonstrate here that cell cortex localized microtubules interact with the division site and are added to the phragmoplast to direct its outward expansion during telophase.

RESULTS

Cell cortex localized telophase microtubules are organized by the division site and distinct from the phragmoplast.

Live-cell imaging of proliferative maize leaf epidermis cells during telophase revealed an unexpected population of microtubules at the cell cortex that were spatially distinct from the phragmoplast. These cell cortex telophase microtubules nucleated from the cell cortex during the anaphase to telophase transition and were present in over 90% of wild type cells during telophase (n =173/190 cells from 26 individual plants). Microtubules in the phragmoplast were identified by close association with the cell plate, labelled with the plasma membrane and cell plate marker FM4-64, and were distinct from telophase cortical arrays. As expected, I observed that microtubules in the phragmoplast were organized into antiparallel, disk or ring shaped, arrays in both wild type and *tangled1* mutant cells. In wild type, cell cortex telophase microtubule arrays covered 33 +/- 2% of the proximal cell face and were typically arranged into two anti-parallel arrays perpendicular to the division plane with an average anisotropy of 0.11 +/- 0.01 (n =38 microtubule arrays from 19 cells of 7 plants). The anisotropy values we observed were similar to meristematic Arabidopsis interphase microtubule arrays (Boudaoud et al. 2014). We also observed cell cortex telophase microtubules in

Arabidopsis root cells, similar to previously published images of Arabidopsis root cells (Kong et al. 2010).

TANGLED1 is a division site localized protein that is required for proper phragmoplast guidance and expansion (Martinez et al. 2017; Walker et al. 2007; Mir et al. 2018; Smith et al. 2001). TANGLED1 has been observed crosslinking and bundling microtubules independent of contact angle in vitro (Martinez et al. 2019). We hypothesized that loss of TANGLED1 would lead to defects in organization of the cell cortex telophase microtubule array. We observed that cell cortex telophase microtubules were completely absent in 20% of *tangled1* mutant cells (n =24/122 cells from 24 plants). When cell cortex telophase microtubules were present, we observed that they were less dense and less evenly distributed across the proximal cell surface (n=98/122 from 24 plants) (Figure 2.1B). Further, the orientation ($P < 0.0001$) and anisotropy ($P = 0.0054$) of these arrays was significantly different in *tangled1* mutants compared to wild type (Figure 2.1C-E).

To understand how cell cortex telophase microtubules formed arrays perpendicular to the division plane, we examined individual microtubule dynamics as microtubules approached the putative division site. In wild type cells, we observed that microtubules were transiently stabilized by pausing at the

division site. When cell cortex telophase microtubules touched the division site they paused 77% of the time (n = 69/90 microtubules from 5 cells of 3 plants), underwent immediate catastrophe 13% of the time and passed through the division site 10% of the time. The median pause time was 33.43 seconds at the division site, and 13.01 seconds in other locations. When growth speeds were measured, there was no difference between microtubules growing toward the division site or in any other direction. My hypothesis is that the transient stabilization of cell cortex telophase microtubules at the division site promoted the overall perpendicular orientation of the arrays. In contrast to wild type cells, cell cortex telophase microtubules were not transiently stabilized at the division site compared to elsewhere in *tangled1* mutants (n = 38 microtubules from 5 cells of 3 plants), even though the overall median microtubule pause time did increase to 58.06 seconds. Additionally, the majority of microtubules, 76%, grew past the division site in *tangled1* mutant cells, only 24% of microtubules paused and no microtubules underwent immediate catastrophe. Taken together, this data suggests that TANGELD1 is essential for proper cell cortex telophase microtubule array organization and promotes both microtubule pausing and shrinking at the division site.

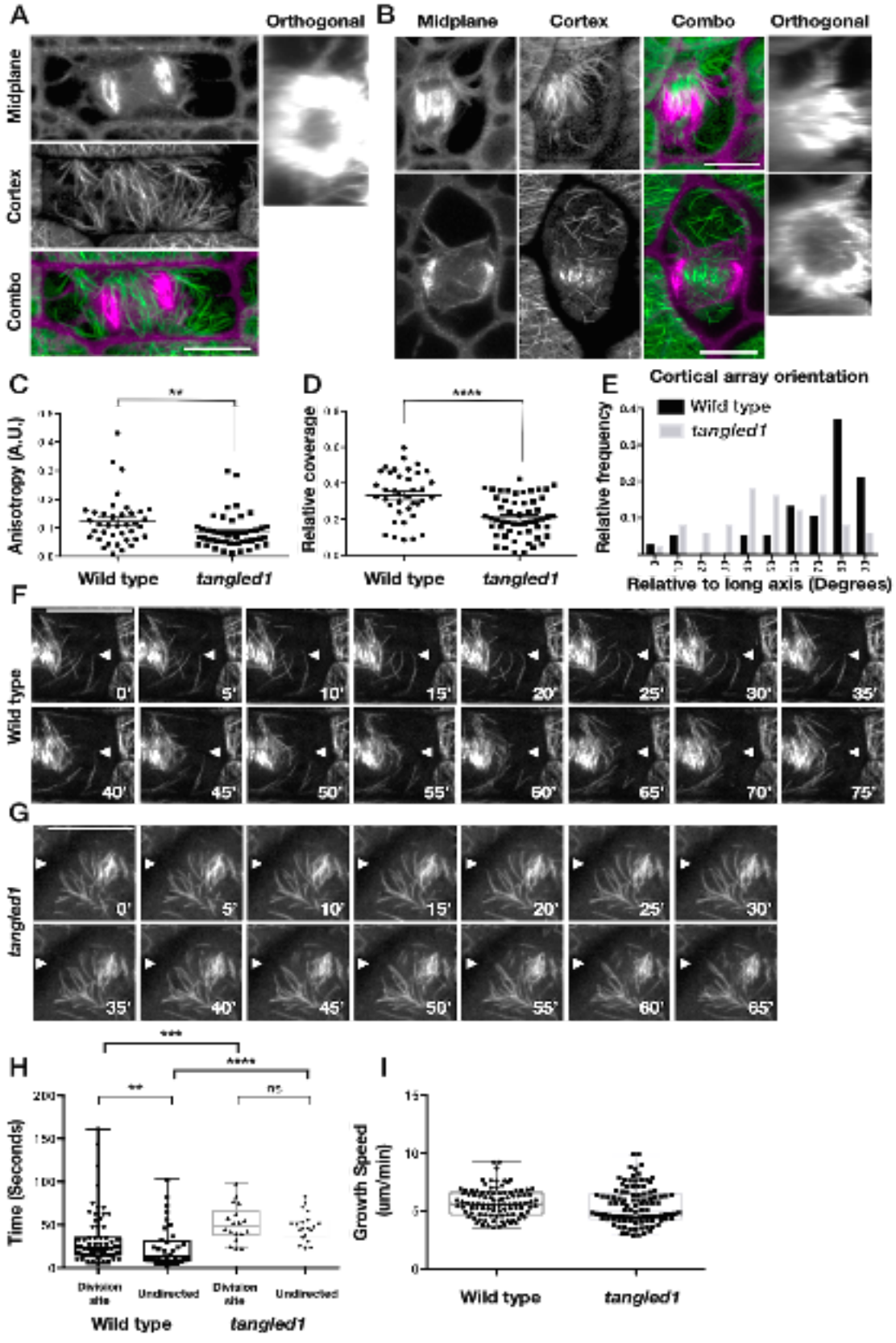
A
Orthogonal
Midplane
Cortex
Combo
B
Midplane
Cortex
Combo
Orthogonal
C
Anisotropy (A.U.)
Wild type
tangled1
D
Relative coverage
Wild type
tangled1
E
Cortical array orientation
Wild type
tangled1
Relative frequency
Relative to long axis (Degrees)
F
Wild type
0'
5'
10'
15'
20'
25'
30'
35'
40'
45'
50'
55'
60'
65'
70'
75'
G
tangled1
0'
5'
10'
15'
20'
25'
30'
35'
40'
45'
50'
55'
60'
65'
H
Time (Seconds)
Division site
Undirected
Division site
Undirected
Wild type
tangled1
I
Growth Speed (um/min)
Wild type
tangled1

Figure 2.1 The organization of cell cortex telophase microtubule arrays in wild type and *tangled1* mutant cells. (A) Micrographs of a wild type cell during telophase from the midplane (top panel) and cell cortex (middle panel). Both the midplane (magenta) and cell cortex (green) sections were overlaid in the bottom panel. An orthogonal view (right panel) of the phragmoplast. Microtubules are marked by YFP-TUBULIN. Scale bar is set to 10 μm. Similar results were observed in 173 cells from 26 plants. (B) Micrographs of a *tangled1* cells during telophase from the midplane (left panel) and cell cortex (middle panel). The midplane (magenta) and cell cortex (green) sections were overlaid in the right panel. An orthogonal view (far-right panel) of phragmoplasts. Microtubules are marked by YFP-TUBULIN. Scale bar is set to 10 um. Similar results were observed in 98 cells from 24 plants. (C) Dot plots of cell cortex telophase microtubule array anisotropy. The median value for wild type cells (0.11 +/- 0.01 A.U.) was calculated using 38 microtubule arrays from 19 cells of 7 plants. The median value for *tangled1* mutant cells (0.07 +/- 0.01 A.U.) was calculated using 50 microtubule arrays from 25 cells of 9 plants. The difference in microtubule array anisotropy is considered significant using a Mann-Whitney test, $P = 0.0054$. (D) Dot plots of telophase microtubule array percent coverage across the proximal cell cortex. The median value for wild type cells (0.33 +/- 0.02) was calculated using 38 microtubule arrays from 19 cells of 7 plants. The median value for *tangled1* mutant cells (0.20 +/- 0.01) was calculated using 50 microtubule arrays from 25 cells of 9 plants. The difference in microtubule array percent coverage is considered significant using a Mann-Whitney test, $P < 0.0001$. (E) Bar graph of telophase microtubule array angle distributions. The median value for wild type cells (79 +/- 4 Degrees) was calculated using 38 microtubule arrays from 19 cells of 7 plants. The median value for *tangled1* mutant cells (50 +/- 3 Degrees) was calculated using 50 microtubule arrays from 25 cells of 9 plants. The difference in microtubule array orientation is considered significant using a Mann-Whitney test, $P < 0.0001$. The distribution of microtubule array orientations is considered significantly different using an F-test, $P = 0.01$. (F) Micrographs of a wild type cell during telophase. Images were captured every 5 seconds for 75 seconds. Scale bar is set to 5um. Similar results were observed in 12 cells from 8 plants. (G) Micrographs of a *tangled1* cell during telophase. Images were captured every 5.04 seconds for 65 seconds. Scale bar is set to 5 μm. Similar results were observed in 15 cells from 6 plants. White arrow indicates the positions of microtubule contact with the cell wall. Micrographs of microtubules marked by YFP-TUBULIN at the cell cortex during telophase were used for calculating anisotropy, microtubule array orientation and percent coverage. (H) Dot plots of cell cortex telophase microtubule pause times at the division site or elsewhere in the cell. Values were calculated by tracking individual microtubule growth trajectories and counting the number of frames a microtubule spent in residence at a single location. The median value for

microtubule pause time at the division site is 22.7 +/- 3.7 seconds in wild type cells and 49.1 +/- 5.0 seconds in *tangled1* mutant cells. The difference in microtubule pause time at the division site is considered significant using a Mann-Whitney test, P = 0.0002. Values for wild type cells were calculated using 68 microtubules from 5 cells of 3 plants. Values for *tangled1* cells were calculated using 18 microtubules from 5 cells of 3 plants. The median value for microtubule pause time not at the division site is 13.0 +/- 3.9 seconds in wild type cells and 46.6 +/- 3.8 seconds in *tangled1* mutant cells. Values for wild type cells were calculated using 38 microtubules from 5 cells of 3 plants. Values for *tangled1* cells were calculated using 20 microtubules from 5 cells of 3 plants. There was a significant difference between pause times at the division site or elsewhere in the wild type cells, using a Mann-Whitney test, P = 0.0095. There was no significant difference between pause times at the division site or elsewhere in the *tangled1* mutant cells. (I) Dot plots of cell cortex telophase microtubule growth speed in wild type and *tangled1* mutant cells. Values were calculated by tracing a line over a kymograph and measuring the slope. Kymographs of microtubule growth were obtained by tracing a line over a microtubule during its growth phase and using the Multi kymograph function in FIJI. The median microtubule growth speed in wild type cells (5.71 +/- 0.12 μm/min) was calculated using 100 microtubules from 5 cells of 3 plants. The median value for *tangled1* mutant cells (5.49 +/- 0.16 μm/min) was calculated using 105 microtubule arrays from 5 cells of 3 plants. The difference in microtubule array growth speed in wild type or *tangled1* mutant cells was not considered significantly different using a Mann-Whitney test.

Cell cortex telophase microtubules are added to the phragmoplast.

I observed cortical microtubules during telophase as they interacted with the division site as well as the phragmoplast. I counted 545 total microtubules in wild types cells (n = 5 cells from 3 individual plants) at the cortex during a 250 second time window during telophase. In wild type cells I observed that nearly half of the microtubules interacted with the phragmoplast (n =251/545 microtubules). When these microtubules contacted the phragmoplast, 78% (n =197/251 microtubules) were incorporated into the phragmoplast, while the remaining 22% underwent immediate catastrophe. Most (66%) microtubule interactions with the phragmoplast occured at the leading edge and resulted in incorporation by parallel bundling. Following a bundling event, I observed that 47% of the microtubules that became incorporated were severed, with a median simultaneous interaction time of 42.28 seconds. These severing events separated the microtubule from the cell cortex and promoted the permanent addition of new microtubules near the phragmoplast leading edge. KATANIN-mediated severing directed by the phragmoplast localized microtubule-binding protein, MACET4/CORD4 may be responsible for organizing microtubules added to the phragmoplast via cell cortex localized microtubules during telophase (Schmidt and Smertenko 2019; Sasaki et al. 2019). I observed simultaneous interactions with the cell cortex and phragmoplast that persisted through the end of the time series in the remaining 53% of microtubules.

I also observed cell cortex telophase microtubules interacting with the phragmoplast in *tangled1* mutant cells (n = 163/591 microtubules in 5 cells from 3 individual plants). Similar to wild type, I observed that these microtubules interacted with and became incorporated into the phragmoplast. In contrast to wild type, fewer (28%) cortical microtubules interacted with the phragmoplast. Interestingly, more of the microtubules that interacted with the phragmoplast from the cell cortex became incorporated via parallel bundling (90%). Additionally, more of these microtubules were severed and then incorporated into the phragmoplast (62%) and also had a longer median simultaneous interaction time (60.43 seconds). This data shows that cell cortex localized microtubules are added to the phragmoplast in both wild type and *tangled1* mutant cells.

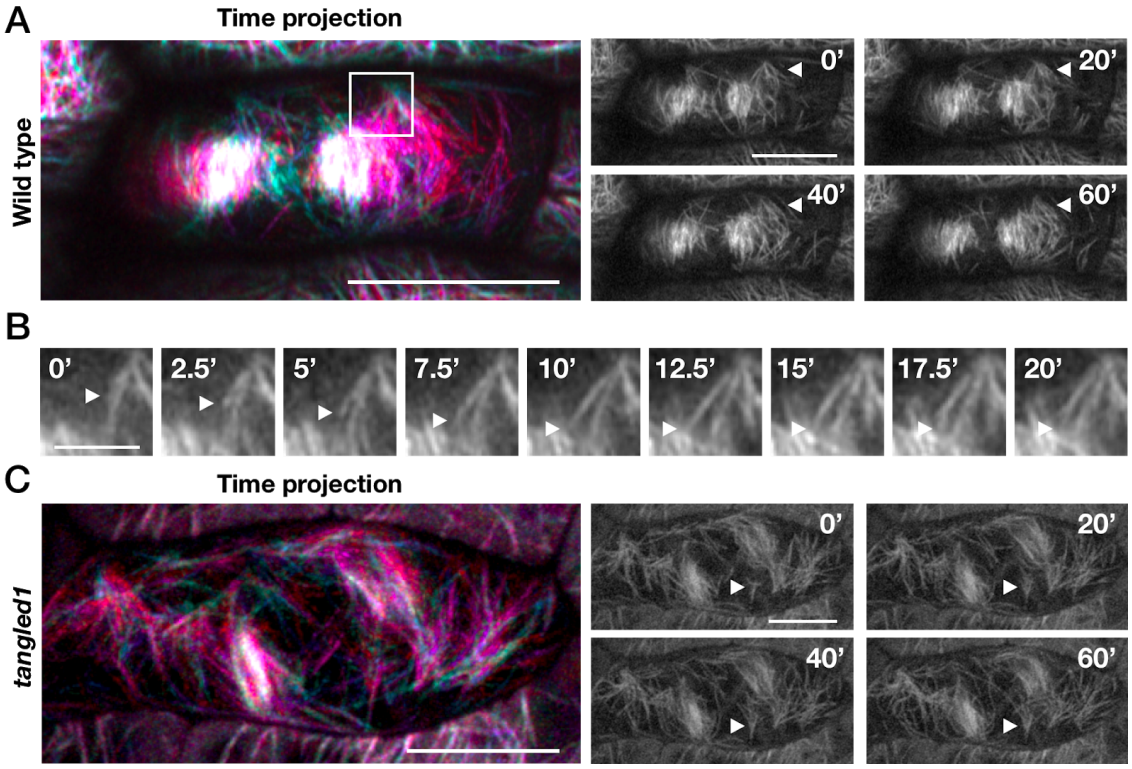
A
Time projection
Wild type
0’
20’
40’
60’
B
0’
2.5’
5’
7.5’
10’
12.5’
15’
17.5’
20’
C
Time projection
tangled1
0’
20’
40’
60’

Figure 2.2 Cell cortex telophase microtubule interaction and bundling events in wild type and *tangled1* mutant cells. (A) Micrographs of a wild type cell during telophase from the cell cortex. Images were captured every 2.52 seconds for 250 seconds and overlaid into a color-coded time projection in the left panel. Time is displayed in seconds. White arrows point to cell cortex telophase microtubules. Microtubules are marked by YFP-TUBULIN. Scale bar is set to 10um. Similar results were observed in 12 cells from 8 plants. (B) Micrographs of cell cortex telophase microtubules nucleating new microtubules and interacting with the phragmoplast in a wild type cell during telophase. Images were captured every 2.52 seconds for 20 seconds. Scale bar is set to 2um. Arrow indicates growing microtubule plus-end. Similar results were observed from >300 microtubules in 27 cells from 14 wild type or *tangled1* mutant plants. (C) Micrographs of a *tangled1* cell during telophase from the cell cortex. Images were captured every 2.52 seconds for 250 seconds and overlaid into a color-coded time projection in the left panel. Microtubules at earlier time points appear blue. Microtubules at later time points appear magenta. Microtubules at all time points appear white. Time is displayed in seconds. White arrows point to cell cortex telophase microtubules. Microtubules are marked by YFP-TUBULIN. Microtubules at earlier time points appear blue. Microtubules at later time points appear magenta. Microtubules at all time points appear white. Micrographs of a single time point within the time series are shown in panels on the right. Scale bar is set to 10um. Similar results were observed in 12 cells from 8 plants.

A

	Phragmoplast trailing edge			Phragmoplast leading edge		
Sample	Time bundled (Seconds, mean +/- SEM)	Angle bundled (Degrees, mean +/- SEM)	Proportion of microtubules (%, n)	Time bundled (Seconds, mean +/- SEM)	Angle bundled (Degrees, mean +/- SEM)	Proportion of microtubules (%, n)
Wild type	45.75 +/- 6.781	26.57 +/- 1.804	34 (86)	108.6 +/- 6.922	21.48 +/- 1.113	66 (166)
tangled1	****63.07 +/- 6.305	28.44 +/- 1.901	**47 (77)	97.96 +/- 7.745	25.14 +/- 2.032	**53 (86)
P value	0.0001	ns	0.0074	ns	ns	0.0074

B

	Phragmoplast interaction types				Division site interaction types			
Sample	Depolymerized (%, n)	Stayed (%, n)	Severed (%, n)	Stabilized (%,n)	Growth across division site (%, n)	Pause at division site (%, n)	Shrink away from division site (%)	Buckle (%, n)
Wild type	22 (54)	78 (197)	37 (94)	41 (103)	9 (8)	77 (69)	13 (12)	59 (90)
tangled1	**10 (16)	**90 (147)	**56 (92)	34 (55)	76 (29)	24 (9)	0 (0)	57 (38)
P value	0.0019	0.0019	0.002	ns	0.0001	0.0001	0.0017	ns

Table 2.1 Quantification of individual interaction and bundling events between cell cortex telophase derived microtubules and the phragmoplast. (A) Summary of cell cortex derived microtubule bundling times and angles with the phragmoplast. (B) Summary of cell cortex derived microtubule interact types with the phragmoplast or putative division site. (B) Significance was determined using a Fisher's exact-test and indicated by (**) $P < 0.01$, (****) $P < 0.0001$.

The asymmetric addition of cell cortex telophase microtubules into the phragmoplast guides it toward the division site.

Next I wondered if the addition of cell cortex telophase microtubules could alter the direction of phragmoplast expansion by guiding the phragmoplast toward the division site. I created kymographs by tracing lines over the cell cortex at the region where phragmoplast expansion was occuring in a time series (Figure 2.3A). Two lines were traced over the phragmoplast midzone (on either side) and two lines were traced exactly above or below the first set of lines. The lines at the phragmoplast midzone show where the kymographs tracked phragmoplast expansion on opposite sides of the cell plate. The second set of lines show where the kymographs recorded microtubule crossover from the cell cortex telophase microtubule array to the phragmoplast. I observed that microtubules from the cell cortex telophase microtubule array crossed toward the phragmoplast near the leading edge (Figure 2.3B). This result was similar to and agreed with my previous result that individual microtubule interaction and bundling occurs primarily at the leading edge of the phragmoplast in wild type cells. Additionally, I found that microtubules from the cell cortex telophase array crossed over toward the phragmoplast at unequal amounts on one side of the cell during the time series (Figure 2.3B & C). The side of the cell that showed more microtubule crossover also displayed a noticeable change in the direction of phragmoplast expansion (Figure 2.3A). On average I saw a 4.2 degree change

in phragmoplast angle every 30 seconds (n > 500 time intervals from 7 wild type cells and 4 *tangled1* cells) at the phragmoplast midzone. This result suggests that cell cortex telophase microtubules can alter the direction of phragmoplast expansion.

Next, I wanted to understand how asymmetric microtubule addition from the cell cortex affected phragmoplast guidance over a longer period of time. I imaged wild type and *tangled1* mutant cells at the cell cortex during telophase every 30 seconds for 30 minutes (n > 500). I measured the angle of the phragmoplast midplane (Figure 2.3A & D) and the asymmetric distribution of cell cortex telophase microtubules near the phragmoplast at each time point (Figure 2.3E). I plotted the measurements as seperate lines from the same time series and analyzed the results using a cross-correlation function. I found that there was a significant correlation between the change in cell cortex telophase microtubule array asymmetry and the change in phragmoplast midplane orientation (Figure 2.3F). This data also revealed that there was an average offset of 102 seconds from the time that microtubule array asymmetry changed to the time that phragmoplast midplane orientation changed (n = 7 wild type cells). This result suggests that cell cortex telophase microtubules can alter the direction of phragmoplast expansion and that there is a lag time of almost 2 minutes between the time of bundling and phragmoplast reorientation.

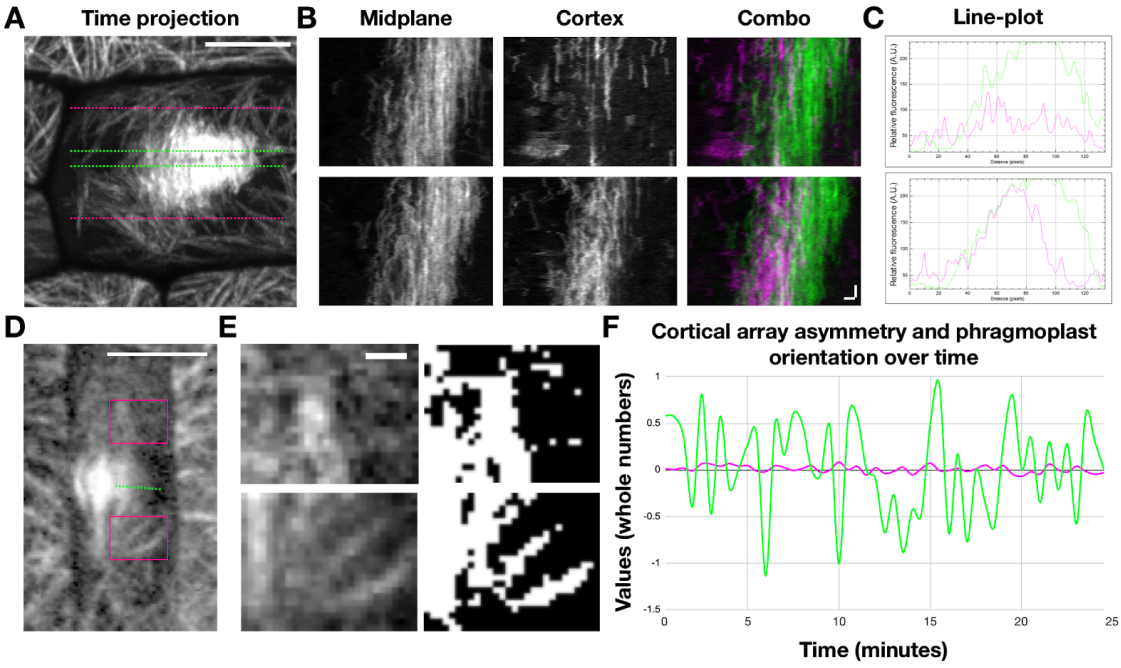
A
Time projection
B
Midplane
Cortex
Combo
C
Line-plot
D
E
F
Cortical array asymmetry and phragmoplast orientation over time
Values (whole numbers)
Time (minutes)

Figure 2.3: The asymmetric addition of cell cortex telophase microtubules alters the direction of phragmoplast expansion. (A) Micrographs of a wild type cell during telophase from the cell cortex. Images were captured every 2.5 seconds for 250 seconds and overlaid into a time projection. Lines were traced over the cell cortex near the phragmoplast midplane (green) and at a location where cortical telophase microtubules crossed over to interact with the phragmoplast (magenta), and were used to generate kymographs. Scale bar is set to 5um. (B) Kymographs of microtubules near the phragmoplast midplane (left panels, green), cross-over locations (middle panels, magenta) and paired (top or bottom) then combined (right panels). Line-plots of relative fluorescence intensities of microtubules near the phragmoplast midplane (green) and a location where cortical microtubules crossed over to interact with the phragmoplast (magenta). Relative fluorescence is measured in arbitrary units and plotted on the Y-axis. Space is measured in pixels and plotted on the X-axis. Horizontal scale bar is set to 1 μm. Vertical scale bar is set to 20 seconds. Similar results were observed in 12 wild type cells and 15 *tangled1* cells. (D) Micrograph of a cell during telophase. Boxes (magenta) are regions of interest at the cell cortex. Dotted line (green) is the phragmoplast midplane. Scale bar is set to 10 μm. (E) Micrographs of cell cortex telophase microtubules above (left, top panel) or below (left, bottom panel) the phragmoplast. Threshold (right panels) of micrographs (left panels) used for asymmetric microtubule array distribution analysis at the cell cortex, either above (top panel) or below (bottom panel) the phragmoplast. Scale bar is set to 1 μm. (F) Line-plot of telophase cell cortex microtubule array asymmetry (magenta) and phragmoplast midplane orientation (green) over time. Percent difference in microtubule array coverage and the $\log_{10}$ of phragmoplast midplane orientation (magenta) over time is quantified as a whole number. Time is on the X-axis and phragmoplast orientation and microtubule array asymmetry are on the Y-axis. The time interval for line-plot data is 30 seconds. Time is displayed in minutes. $P < 0.05$ was determined using the cross-correlation analysis function via the Stats package in R. Similar results were observed in 7 wild type cells and 3 *tangled1* cells. The median offset was 102 seconds for wild type cells and 240 seconds for *tangled1* cells. YFP-TUBULIN was used to mark microtubules.

DISCUSSION

Plants have two unique mitotic microtubule structures, the preprophase band and the phragmoplast (Livanos and Müller 2019). The phragmoplast is responsible for guiding the cell plate as it expands toward the division site (Smertenko 2018). *tangled1* mutant cells have cell shape defects that are best explained by the failure of phragmoplasts to return to the proper division site during telophase and cytokinesis. How the phragmoplast is directed towards the division site by TANGLED1 has been a mystery to plant cell biologists (Livanos and Müller 2019; Rasmussen and Bellinger 2018).

I showed here that cell cortex localized microtubules during telophase are distinct from the phragmoplast and organize perpendicular to the division plane. I found this array was misorganized and diminished, or absent, in *tangled1* mutant cells. My hypothesis was that cell cortex telophase microtubules became organized by TANGLED1 to guide the phragmoplast to the division site. Individual microtubules from the cell cortex telophase microtubule array had altered dynamics at the division site compared to microtubules elsewhere in the cell or in *tangled1* mutants. I also found that microtubules from the cell cortex preferentially interacted with the leading edge of the phragmoplast in wild type cells but this pattern was abolished in *tangled1* mutants. Additionally, microtubules from the cell cortex that bundled with the phragmoplast were

permanently added by severing, likely via MACET/CORD4 anchored KATANIN. Finally, we showed that the asymmetric bundling of cell cortex telophase microtubules had a direct affect on the direction of phragmoplast expansion. Together, these findings describe a possible mechanism for how phragmoplast guidance is achieved by division site localized proteins, like TANGLED1 in maize. Observing this microtubule array in other mutants with known phragmoplast guidance defects may help to shed light on how division plane maintenance is achieved in plants.

MATERIALS AND METHODS

Plant growth and imaging conditions. Maize plants were grown in 1L pots in standard greenhouse conditions, 16-h light, 8-h dark at University of California, Riverside. Maize plants between 3 and 4 weeks old were imaged. Maize plants segregating YFP-TUBULIN, CFP-TUBULIN, TANGLED1-YFP, EB1-mCHERRY or *tangled1* were identified by microscopy or by genotyping. Leaves were removed until the ligule height was <2 mm. Adaxial symmetrically dividing leaf blade samples were mounted in water and covered with Fisherbrand microscope cover glass 24X30-1.5 or loaded into a Rose chamber. Cells were collected from more than 3 plants of each phenotype. The imaging temperature was 23˚C for images captured on the Zeiss LSM880 and 21C for images captured on the custom-built spinning disk from Solamere Technology.

Arabidopsis plants were grown in sterile conditions on ½ xMS plates closed with 3M micropore tape and grown in a chamber at 24˚C, 16-h light, 8-h dark. Arabidopsis plants between 3 and 5 days post germination were imaged. Arabidopsis plants segregating CFP-TUBULIN were identified by microscopy. Whole plants were mounted in water on microscope cover glass 24X30-1.5 (Fisher Scientific). Cells were imaged from > 3 plants. Root epidermal and cortex cells from the meristematic zone were imaged. Images were captured on the Zeiss LSM880 at a temperature of 23˚C.

Confocal microscopy. Fluorescence was recorded using a Zeiss LSM 880 equipped with Airyscan with a 100x objective (NA = 1.46). Images captured using the Zeiss LSM 880 were processed using Airyscan on default settings with ZEN software (Zeiss) or a custom-built spinning disk from Solamere Technology with a Yokogawa W1 spinning disk, EM-CCD camera from Hamamatsu 9100c and Nikon Eclipse TE inverted stand with a 100x, NA - 1.45, objective lens. The stage of the custom-built spinning disk microscope was fully motorized and controlled with Micromanager-1.4 with ASI Peizo, 300µm range, and 3 axis DC servo motor controller. The custom-built spinning disk microscope used solid-state lasers from Obis between 40 to 100mW and standard emission filters from Chroma Technology. For YFP-TUBULIN or TANGLED1-YFP, a 514 laser with emission filter 540/30 was used. For CFP-TUBULIN a 445 laser with emission filter 480/40

was used. For EB1-mCHERRY a 561 laser with emission filter 620/60 was used. Type FF Microscope immersion oil (Cargille was used with 100x objective lenses. Maize leaf epidermis cells during telophase were identified by the presence of a phragmoplast. Images were captured at the cell cortex using adjacent interphase cortical microtubule arrays as a point of reference. Two-dimensional projections, time projections and three-dimensional reconstructions of Z stacks and time-lapse images were generated with Fiji http://rsb.info.nih.gov/ij/. Image color was altered using the linear levels option, color merges and figures were assembled with GIMP-2.10.8 https://www.gimp.org/downloads/. Horizontal drift was corrected in Fiji with StackReg https://imagej.net/StackReg using the translation option. Photo bleaching was corrected in FIJI using the Simple Ratio method.

Time lapse and quantification of microtubule growth, pause and shrinkage. YFP-TUBULIN was used to label the microtubule cytoskeleton. Maize leaf epidermis cells during telophase were identified by the presence of a phragmoplast. A 2.52 second time interval was used. For analysis of microtubule growth and pause, kymographs were created in Fiji as described in (Zanic 2016). All kymographs generated were examined for clear evidence of growth, pause and shrinkage for at least five frames (Lindeboom et al. 2019) and traced by hand. Growth and depolymerization velocities were calculated from kymograph traces. Differences in microtubule growth speed and pause time were analyzed

with PRISM https://www.graphpad.com/ and statistical significance was determined with a Mann-Whitney *U*-test.

Quantification of microtubule array organization, percent coverage and asymmetry. YFP-TUBULIN was used to label the microtubule cytoskeleton. To measure anisotropy, TIFF image files of the cell cortex were converted to PNG files using Fiji software and processed with the FibrilTool plugin (Boudaoud et al. 2014). To measure percent coverage, image files were made binary and thresholded using mean fluorescence and processed using the Area/Volume fraction function with the BoneJ https://imagej.net/BoneJ plugin. Differences in anisotropy and percent coverage were analyzed with PRISM and statistical significance was determined with a Mann-Whitney *U*-test.

Microtubule array asymmetry was calculated by subtracting the cell cortex microtubule array percent coverage above the phragmoplast from the percent coverage below the phragmoplast. Positive values indicated microtubule array asymmetry above the phragmoplast. Negative values indicated microtubule array asymmetry below the phragmoplast. The difference in microtubule array asymmetry at time-point 2 was subtracted from the difference in microtubule array asymmetry at time-point 1. This process was repeated for each point in the time series to obtain the change in microtubule array asymmetry over time.

The direction of phragmoplast expansion was measured by taking the angle of the phragmoplast midplane using the long axis of the cell as a reference. The

phragmoplast midplane angle at time-point 2 was subtracted from the phragmoplast midplane angle at time-point 1. This process was repeated for each point in the time series to obtain the change in phragmoplast orientation over time. Finally, the change in cell cortex telophase microtubule array over time was plotted against the change in phragmoplast expansion direction over time. These values were analyzed for cross-correlation and offset using the Stats package in R. Cells were collected from > 3 plants.

Time lapse of the cell cortex and midplane. YFP-TUBULIN was used to label the microtubule cytoskeleton. Maize leaf epidermis cells during telophase were identified by the presence of a phragmoplast. Images were captured at the cell cortex using adjacent interphase cortical microtubule arrays as a point of reference with a custom-built spinning disk from Solamere Technology. The cell cortex and 4 μm down into the cell for an approximate positioning of the midplane were captured every 30 second seconds. Cells were collected from > 3 plants.

Quantification of microtubule interaction times, angles and types. YFP-TUBULIN was used to label the microtubule cytoskeleton. Maize leaf epidermis cells during telophase were identified by the presence of a phragmoplast. Images were captured at the cell cortex using adjacent interphase cortical microtubule arrays as a point of reference with a Zeiss LSM 880 and processed using Airscan technology. A 2.52 second time interval was used. Microtubules were tracked as they grew from the cell cortex telophase

microtubule array and interacted with the phragmoplast or putative division site. The putative division site was identified by tracing a lines across the cell through the phragmoplast midplane. Microtubules that grew across this line this line were counted as “Growth across the division site”. Microtubules that paused at this line were counted as “Paused”. Microtubules that grew to this line and shrank away from it within one time frame were counted as “Shrank away from division site”. Microtubules that interacted with the division site and buckled were counted as “Buckled”. Microtubule interaction times with the phragmoplast were counted for any cell cortex derived telophase microtubule that stayed in contact with the phragmoplast for more then one time frame. Microtubule interaction angles were measured using microtubules within the phragmoplast as a reference point. Microtubule interactions were considered parallel if plus-ends of two interacting microtubules were facing the same direction. Microtubule interactions were considered anti-parallel if plus-ends of two interacting microtubules were facing opposite directions.

REFERENCES

Boudaoud, Arezki, Agata Burian, Dorota Borowska-Wykręt, Magalie Uyttewaal, Roman Wrzalik, Dorota Kwiatkowska, and Olivier Hamant. 2014. “FibrilTool, an ImageJ Plug-in to Quantify Fibrillar Structures in Raw Microscopy Images.” *Nature Protocols* 9 (2): 457–63.

Chugh, Mayank, Maja Reißner, Michael Bugiel, Elisabeth Lipka, Arvid Herrmann, Basudev Roy, Sabine Müller, and Erik Schäffer. 2018. “Phragmoplast Orienting Kinesin 2 Is a Weak Motor Switching between Processive and Diffusive Modes.” *Biophysical Journal* 115 (2): 375–85.

Cleary, A. L., and L. G. Smith. 1998. “The Tangled1 Gene Is Required for Spatial Control of Cytoskeletal Arrays Associated with Cell Division during Maize Leaf Development.” *The Plant Cell* 10 (11): 1875–88.

Herrmann, Arvid, Pantelis Livanos, Elisabeth Lipka, Astrid Gadeyne, Marie-Theres Hauser, Daniël Van Damme, and Sabine Müller. 2018. “Dual Localized Kinesin-12 POK2 Plays Multiple Roles during Cell Division and Interacts with MAP65-3.” *EMBO Reports*, July. https://doi.org/10.15252/embr.201846085.

Kong, Zhaosheng, Takashi Hotta, Yuh-Ru Julie Lee, Tetsuya Horio, and Bo Liu. 2010. “The γ -Tubulin Complex Protein GCP4 Is Required for Organizing Functional Microtubule Arrays in Arabidopsis Thaliana.” *The Plant Cell*. https://doi.org/10.1105/tpc.109.071191.

Lee, Yuh-Ru Julie, and Bo Liu. 2013. “The Rise and Fall of the Phragmoplast Microtubule Array.” *Current Opinion in Plant Biology* 16 (6): 757–63.

Li, Haoge, Baojuan Sun, Michiko Sasabe, Xingguang Deng, Yasunori Machida, Honghui Lin, Y-R Julie Lee, and Bo Liu. 2017. “Arabidopsis MAP65-4 Plays a Role in Phragmoplast Microtubule Organization and Marks the Cortical Cell Division Site.” *The New Phytologist* 215 (1): 187–201.

Lindeboom, Jelmer J., Masayoshi Nakamura, Marco Saltini, Anneke Hibbel, Ankit Walia, Tijs Ketelaar, Anne Mie C. Emons, et al. 2019. “CLASP Stabilization of plus Ends Created by Severing Promotes Microtubule Creation and Reorientation.” *The Journal of Cell Biology* 218 (1): 190–205.

Liu, Bo, Barry A. Palevitz, and Harish C. Joshi. 1995. “Experimental Manipulation of γ-Tubulin Distribution in Arabidopsis Using Anti-Microtubule Drugs.” *Cell Motility and the Cytoskeleton* 31 (2): 113–29.

Livanos, Pantelis, and Sabine Müller. 2019. “Division Plane Establishment and Cytokinesis.” *Annual Review of Plant Biology*, February. https://doi.org/10.1146/annurev-arplant-050718-100444.

Martinez, Pablo, Ram Dixit, Rachappa S. Balkunde, Seán E. O’Leary, Kenneth A. Brakke, and Carolyn G. Rasmussen. 2019. “TANGLED1 Mediates Interactions between Microtubules That May Promote Spindle Organization and Phragmoplast Guidance to the Division Site in Maize.” *bioRxiv*. https://doi.org/10.1101/711796.

Martinez, Pablo, Anding Luo, Anne Sylvester, and Carolyn G. Rasmussen. 2017. “Proper Division Plane Orientation and Mitotic Progression Together Allow Normal Growth of Maize.” *Proceedings of the National Academy of Sciences of the United States of America* 114 (10): 2759–64.

Mir, Ricardo, Victoria H. Morris, Henrik Buschmann, and Carolyn G. Rasmussen. 2018. “Division Plane Orientation Defects Revealed by a Synthetic Double Mutant Phenotype.” *Plant Physiology* 176 (1): 418–31.

Müller, Sabine, Shengcheng Han, and Laurie G. Smith. 2006. “Two Kinesins Are Involved in the Spatial Control of Cytokinesis in Arabidopsis Thaliana.” *Current Biology: CB* 16 (9): 888–94.

Murata, Takashi, Toshio Sano, Michiko Sasabe, Shigenori Nonaka, Tetsuya Higashiyama, Seiichiro Hasezawa, Yasunori Machida, and Mitsuyasu Hasebe. 2013. “Mechanism of Microtubule Array Expansion in the Cytokinetic Phragmoplast.” *Nature Communications* 4: 1967.

Rasmussen, Carolyn G., and Marschal Bellinger. 2018. “An Overview of Plant Division-Plane Orientation.” *The New Phytologist*, April. https://doi.org/10.1111/nph.15183.

Sasabe, Michiko, and Yasunori Machida. 2012. “Regulation of Organization and Function of Microtubules by the Mitogen-Activated Protein Kinase Cascade during Plant Cytokinesis.” *Cytoskeleton*. https://doi.org/10.1002/cm.21072.

Sasaki, Takema, Motosuke Tsutsumi, Kohei Otomo, Takashi Murata, Noriyoshi Yagi, Masayoshi Nakamura, Tomomi Nemoto, Mitsuyasu Hasebe, and Yoshihisa Oda. 2019. “A Novel Katanin-Tethering Machinery Accelerates Cytokinesis.” *Current Biology: CB*, October. https://doi.org/10.1016/j.cub.2019.09.049.

Schmidt, Sharol, and Andrei Smertenko. 2019. “Identification and Characterization of the Land-Plant-Specific Microtubule Nucleation Factor MACET4.” *Journal of Cell Science* 132 (11). https://doi.org/10.1242/jcs.232819.

Smertenko, Andrei. 2018. “Phragmoplast Expansion: The Four-Stroke Engine That Powers Plant Cytokinesis.” *Current Opinion in Plant Biology* 46 (December): 130–37.

Smertenko, Andrei, Farhah Assaad, František Baluška, Magdalena Bezanilla, Henrik Buschmann, Georgia Drakakaki, Marie-Theres Hauser, et al. 2017. “Plant Cytokinesis: Terminology for Structures and Processes.” *Trends in Cell Biology* 27 (12): 885–94.

Smith, L. G., S. M. Gerttula, S. Han, and J. Levy. 2001. “Tangled1: A Microtubule Binding Protein Required for the Spatial Control of Cytokinesis in Maize.” *The Journal of Cell Biology* 152 (1): 231–36.

Stöckle, Dorothee, Arvid Herrmann, Elisabeth Lipka, Theresa Lauster, Richard Gavidia, Steffi Zimmermann, and Sabine Müller. 2016. “Putative RopGAPs Impact Division Plane Selection and Interact with Kinesin-12 POK1.” *Nature Plants* 2 (August): 16120.

Walker, Keely L., Sabine Müller, Dorianne Moss, David W. Ehrhardt, and Laurie G. Smith. 2007. “Arabidopsis TANGLED Identifies the Division Plane throughout Mitosis and Cytokinesis.” *Current Biology: CB* 17 (21): 1827–36.

Wick, S. M. 1985. “Immunofluorescence Microscopy of Tubulin and Microtubule Arrays in Plant Cells. III. Transition between Mitotic/cytokinetic and Interphase Microtubule Arrays.” *Cell Biology International Reports* 9 (4): 357–71.

Wu, Shu-Zon, and Magdalena Bezanilla. 2014. “Myosin VIII Associates with Microtubule Ends and Together with Actin Plays a Role in Guiding Plant Cell Division.” *eLife* 3 (September). https://doi.org/10.7554/eLife.03498.

Zanic, Marija. 2016. “Measuring the Effects of Microtubule-Associated Proteins on Microtubule Dynamics In Vitro.” *Methods in Molecular Biology* 1413: 47–61.

CHAPTER THREE: KINECTIN is a microtubule organizing protein with an essential role in cell shape determination in plants

ABSTRACT

The ability of plants to produce specific cell shapes is essential for proper growth and development (Sapala et al. 2018). A number of microtubule-associated proteins have essential roles in cell shape determination (Krtková, Benáková, and Schwarzerová 2016). The proper organization of microtubules is important for correct division plane position during mitosis and anisotropic cell expansion during interphase (Kirik et al. 2007). TANGLED1 is a microtubule-associated protein that has been shown to crosslink and bundle microtubules in vitro (P. Martinez et al. 2019). KINECTIN was identified to directly interact with TANGLED1 via a Yeast-2 hybrid screen (Su 2012). In animals, KINECTIN has been shown to alter the activity of a class of microtubule associated KINESIN motor proteins by direct binding (Ong et al. 2000). To better understand the relationship between TANGLED1 and KINECTIN, I characterized *kinectin* loss-of-function mutants via *CRISPR*/CAS9 mediated mutagenesis in maize (Ausubel et al. 2001). I found that *kinectin* mutant cells were smaller and had more isotropic cell shapes. This phenotype was exacerbated and caused defects in mesocotyl elongation when plants were grown in the dark. Additionally, microtubule dynamics and organization at the cell cortex was altered in *kinectin*

mutant cells throughout the cell cycle. Although I did not observe any obvious defects in division plane positioning in *kinectin* mutant cells, there was a significant increase in TANGLED1 accumulation within the metaphase spindle. These results suggest that KINECTIN has an essential role in cell shape determination via a microtubule organization function in plants.

INTRODUCTION

The proper organization of microtubules is essential for normal growth and development (Horio and Murata 2014; Paredez, Somerville, and Ehrhardt 2006; Buschmann et al. 2009; Nakamura, Ehrhardt, and Hashimoto 2010; Komis et al. 2017). The *tangled1* mutant in maize has altered patterns of microtubule organization at the cell cortex during mitosis and defective guidance of a plant specific microtubule structure, the phragmoplast (Smith, Hake, and Sylvester 1996; Cleary and Smith 1998). This mutant phenotype leads to aberrant cell shapes, cell file organization and plant growth defects. While it was reported some time ago that TANGLED1 is a microtubule associated protein in plants (Smith et al. 2001), it was only recently demonstrated that TANGLED1 can crosslink and bundle microtubules in a direction indepedent manner in vitro (P. Martinez et al. 2019). TANGLED1 accumulates at the division site with the maturing preprophase band and remains at this position following preprophase band disassembly (Walker et al. 2007; Rasmussen, Sun, and Smith 2011).

Although TANGLED1 requires the microtubule-dependent motor protein POK1 and POK2 to remain at the division site following preprophase band disassembly, this mechanism occurs via a microtubule-independent pathway (Walker et al. 2007). In an effort to better understand how TANGLED1 remains at the division site throughout mitosis it is necessary to identify and characterize additional TANGLED1 interacting proteins.

KINECTIN was shown to directly interact with TANGLED1 via a yeast-two-hybrid experiment (Su 2012). Previous studies in animals have reported that KINECTIN directly binds and modulates the activity of KINESIN proteins (Ong et al. 2000; Toyoshima et al. 1992; Kumar, Yu, and Sheetz 1995). In Arabidopsis protoplast cells, KINECTIN1 was shown to interact with TUBULIN (Park et al. 2014). Additionally, vacuolar maturation and seedling germination was slow in *kinectin1* loss-of-function mutants (Kwon et al. 2018). Intriguingly, neither of these studies discussed a role for KINECTIN in microtubule organization or cell shape determination. Here, we used maize and Arabidopsis to further characterize the function of KINECTIN in plants. My original hypothesis was that KINECTIN would be important for maintaining TANGLED1 at the division site during mitosis and that loss-of-function *kinectin* mutants would have cell shape defects via aberrant division plane positioning.

RESULTS

KINECTIN retains its KINESIN protein interaction domain and likely functions by mediating protein-protein interactions in plant cells.

KINECTIN is a well characterized integral endoplasmic reticulum and KINESIN-interacting protein in animal cells (Kumar, Yu, and Sheetz 1995; Ong et al. 2000; Toyoshima et al. 1992; Lin, Sun, and Hu 2012). Astonishingly, KINECTIN is conserved between plants and animals. To better understand the function of KINECTIN in plant cells I first compared the amino acid sequence of human KINECTIN to maize (Fig 3.1A). Current plant versions of KINECTIN amino acid sequences had no conserved transmembrane domain. However, the protein-protein interaction domain that is essential for mediating the KINECTIN-KINESIN interaction has a region of shared sequence identity. When run through the NCBI online database as well, similar results were returned for conserved protein domains at the KINECTIN-KINESIN interaction region. This result suggests that KINECTIN-KINESIN interaction may be conserved in plants.

KINECTIN was shown to interact with TUBULIN in Arabidopsis protoplast cells using Bimolecular fluorescence complementation experiments (BiFC or Split YFP) (Park et al. 2014). However, I did not find a conserved microtubule binding domain in any of the amino acids sequences from plants (n = 90) (Supplementary Fig 3.2). Instead, there is a conserved set of three coiled-coil

domains linked by regions of non-structured sequences. It was previously reported that the second and third coiled-coil domains are essential for a KINECTIN-KINASE interaction in *Mesembryanthemum crystallinum* (Chehab, Patharkar, and Cushman 2007). I found that the second and third coiled-coil domains are 100% conserved among current versions of plant sequences (Supplementary Fig 3.2). This data suggests that KINECTIN indirectly interacts with microtubules via microtubule-associated protein interactions in plants.

In Arabidopsis, the *kinectin1* single mutant was reported to have a mild vacuole-related phenotype that caused protein storage vacuoles to delay their transition into lytic vacuoles in seedlings (Kwon et al. 2018). Additionally, subcellular localization and protein-protein interactions have been previously described (Park et al. 2014; Chehab, Patharkar, and Cushman 2007; Kwon et al. 2018). However, these reports showed vesicular localization in fixed *Mesembryanthemum crystallinum* cells and Arabidopsis protoplasts.

To analyze patterns of KINECTIN subcellular localization further, I transformed Arabidopsis plants with a set of fluorescent protein reporters. The cauliflower mosaic virus 35S promoter was used to constitutively express *KINECTIN* in Arabidopsis. Over-expression of *KINECTIN* produced no obvious growth defects in Arabidopsis. YFP-KINECTIN expression was uniform across all cell files in the

root (Fig 3.1D). By comparison, a native promoter driven KINECTIN-YFP reporter line showed expression in all cell types in the root, except in protoxylem cells where higher than average expression was observed (Supp Fig X). The specific position of the YFP reporter with respect to either the N-terminal or C-terminal side of the KINECTIN protein produced no obvious change in the cytosolic and nuclear localization of the protein (Fig 3.2, Supplementary Fig 3.1). To confirm these results, similar patterns of subcellular localization were also observed in stably transformed tobacco BY2 cells (Supplementary Fig 3.1A & B) and transiently transformed tobacco leaves (Supplementary Fig 3.1C & D). YFP-KINECTIN signal was strongest in the cytosol near golgi stacks (Fig. 3.2B) however, there was no evidence to suggest that KINECTIN colocalized with microtubules. Dividing Arabidopsis root epidermis cells were also observed. Here, YFP-KINECTIN signal was increased in the spindle and phragmoplast. This data shows that KINECTIN is a cytosolic protein that is expressed throughout the cell cycle and in many cell and tissue types (Fig 3.1D-F). Interestingly, YFP-KINECTIN signal was strongest in the cytosol near golgi stacks, a region important for KINSEN-vesicle docking and intracellular transport in the cell (Lee, Ohlson, and Pfeffer 2015). Based on this data, it does not appear that KINECTIN is a division site-specific protein in plants.

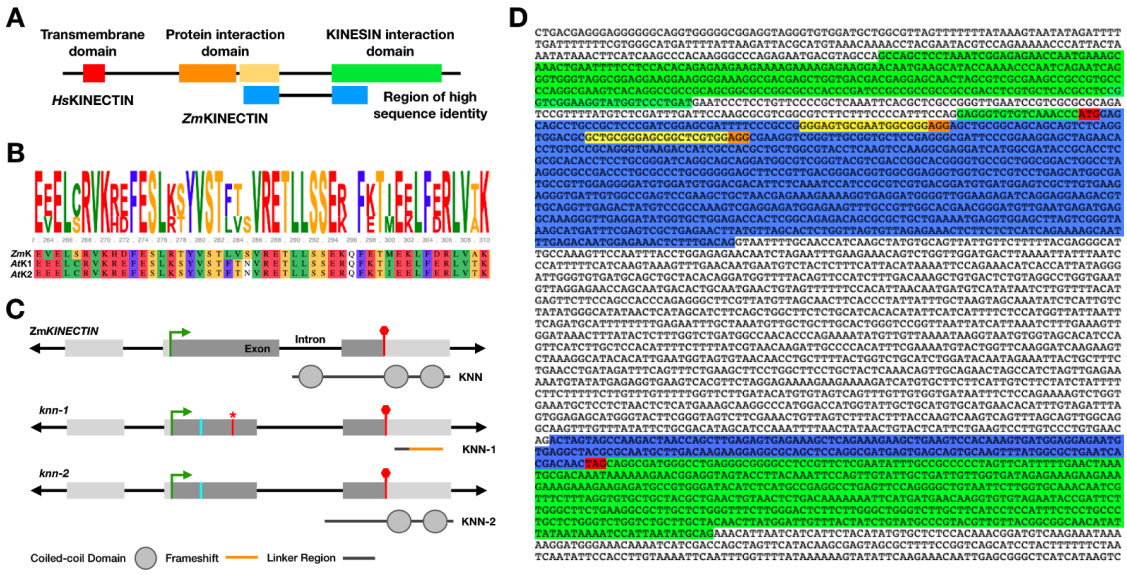

Figure 3.1 Sequence conservation and target site mutagenesis of *KINECTIN* in maize. (A) A cartoon diagram of *Homo sapiens* KINECTIN and the conserved protein domains with relative positions. The transmembrane domain is shown in red, protein interaction domains are shown in orange and yellow, the KINESIN protein interaction domain is shown in green. The overlapping region of sequence identity for *Zea mays* KINECTIN is shown in blue. (B) A region of shared amino acid sequence identity between *Zea mays* KINECTIN and two forms of *Arabidopsis thaliana* KINECTIN. (C) Cartoon diagrams of the KINECTIN gene and two mutant alleles that were generated via *CRISPR*/CAS9. Light grey boxes are untranslated exons. Dark grey boxes are translated exons. Black lines between boxes are introns. Green arrows indicate translational start sites. Blue bands indicate the positions of *CRISPR*/CAS9 mutagenesis. Red stop signs indicate the translational stop site. Red star indicates an early stop following mutagenesis. Ball and stick diagrams of coiled-coil domains connected by regions of unstructured amino acid sequences are displayed below each gene model. (D) *Zea mays KINECTIN* DNA sequence. Untranslated exons are highlighted in green. Translated exons are highlighted in blue. The translational start and stop sites are highlighted in red. *CRISPR*/CAS9 target sites are highlighted in yellow. CAS9 PAM sites are highlighted in orange. Introns and unscribed regions are left unhighlighted.

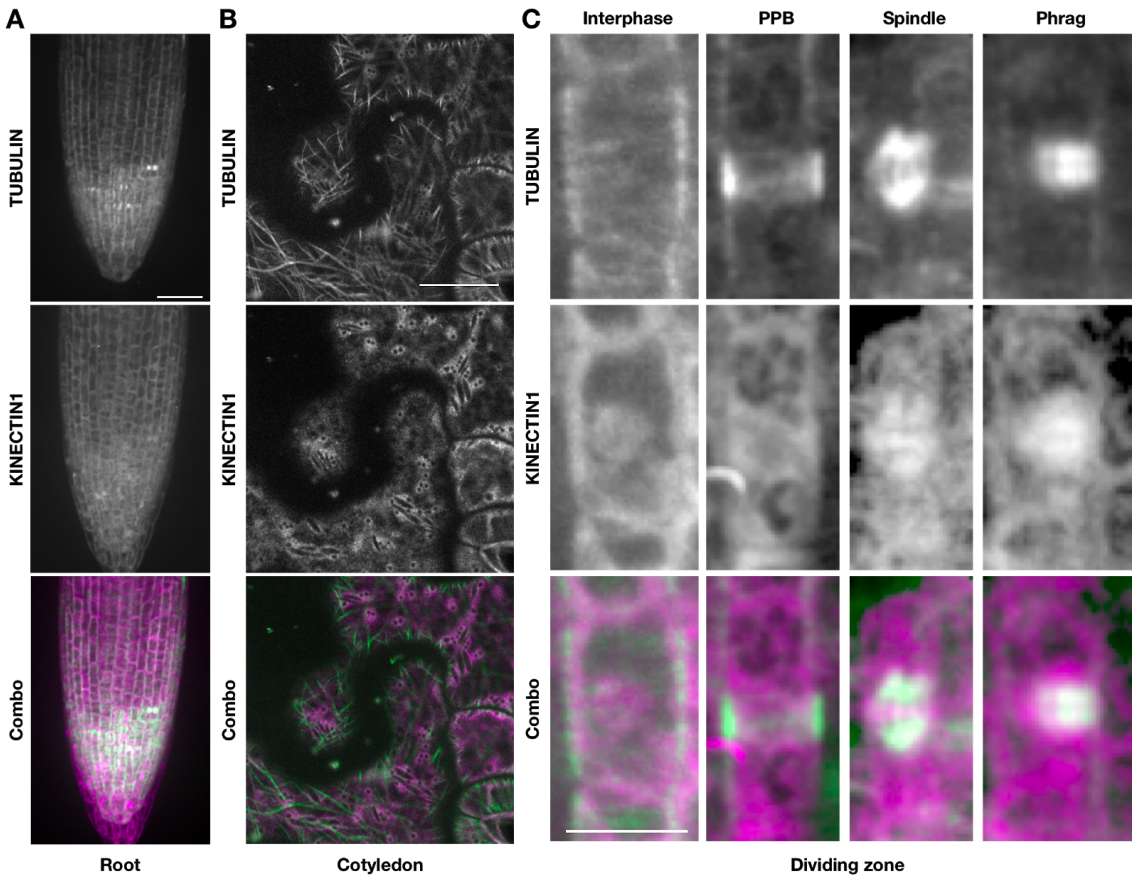

Figure 3.2 KINECTIN1 localization in Arabidopsis. (A) 35S:YFP:KINECTIN1 (magenta) and 35S:CFP:αTUBULIN6 (green) expression in an Arabidopsis root. Scale bar is 50 μm. Similar results were observed in >5 plants. (B) 35S:YFP:KINECTIN1 and 35S:CFP:αTUBULIN6 expression at various stages of mitosis in Arabidopsis root epidermis cells. Scale bar is 5 μm. Similar results were observed in >5 cells of each stage of mitosis from >3 plants. (C) 35S:YFP:KINECTIN1 and 35S:CFP:αTUBULIN6 expression in Arabidopsis leaf epidermal cells. Scale bar is 100 μm. Similar results were observed in >5 plants.

The first coiled-coil domain of the KINECTIN protein is required for proper cell expansion in maize.

Together with a collaborator, Professor Bing Yang at the Danforth Center, we used *CRISPR*/CAS9 to target the single copy *KINECTIN* gene for mutagenesis in maize (Fig 3.1D). The selected target sites flanked either side of the first coiled-coil domain (Fig 3.1C). I chose a set of mutated *kinectin* alleles that represented putative loss-of-functions and either an in-frame deletion of the first coiled-coil domain or a deletion of the second and third coiled-coil domain for further analysis (Fig 3.1C). The *kinectin-1* allele was by far the most common (21%) mutation that we observed (n = 8/38). All results presented below were generated using the *kinectin-1* allele, unless otherwise stated.

I first wanted to know if *kinectin* mutant plants displayed division plane orientation defects in maize. Matched samples (n = 17 plants) from the expanded region of mature leaves were collected, then fixed and stained with toluidine blue O (Fig 3.2A). There was no difference in the rate of division plane defects in *kinectin* cells compared to wild type (n = 1,286 *kinectin* cells and 1,424 Wild type cells). However, the median leaf pavement cell area was significantly smaller in *kinectin* cells (15,600 um^2, n = 916 cells) compared to (17,200 um^2, n = 1,001 cells) wild type (Fig 3.2C).The specific dimension of the cells were analyzed and it was revealed that *kinectin* cells had smaller median lengths (220 μm) across the

longitudinal axis exclusively (Fig 3.2D). This data reveals that *kinectin* mutants express mild cell shape defects in adult plants.

Although the *kinectin* mutants had no obvious division plane orientation defect in the fully expanded regions of the leaf, there was a significant difference in the size of *kinectin* mutant pavement cells across the longitudinal axis. This data supports a hypothesis that *kinectin* mutant cells have expansion defects. To test this hypothesis, I germinated and grew maize seedlings segregating the *kinectin* allele in the dark. Mesocotyl growth in the dark is primarily driven by cell expansion during interphase (Schopfer, Lapierre, and Nolte 2001). Defects in mesocotyl elongation in dark grown maize seedlings can reveal cell expansion defects. The *kinectin* mutants had a median mesocotyl length of 4.8 cm (Fig 3.2 B&G). This was significantly ($P = 0.0105$) shorter than wild type (6.5 cm, $n = 18$ plants) and heterozygotes (5.9 cm, $n = 47$ plants). The *kinectin-2* mutants did not have a noticeable mesocotyl elongation defect (Supplemental Fig. 3.3). Taken together, this data shows that the first coiled-coil domain is essential for KINECTIN cell expansion function. In addition, KINECTIN has a role in cell shape determination but not in cell division plane positioning in maize.

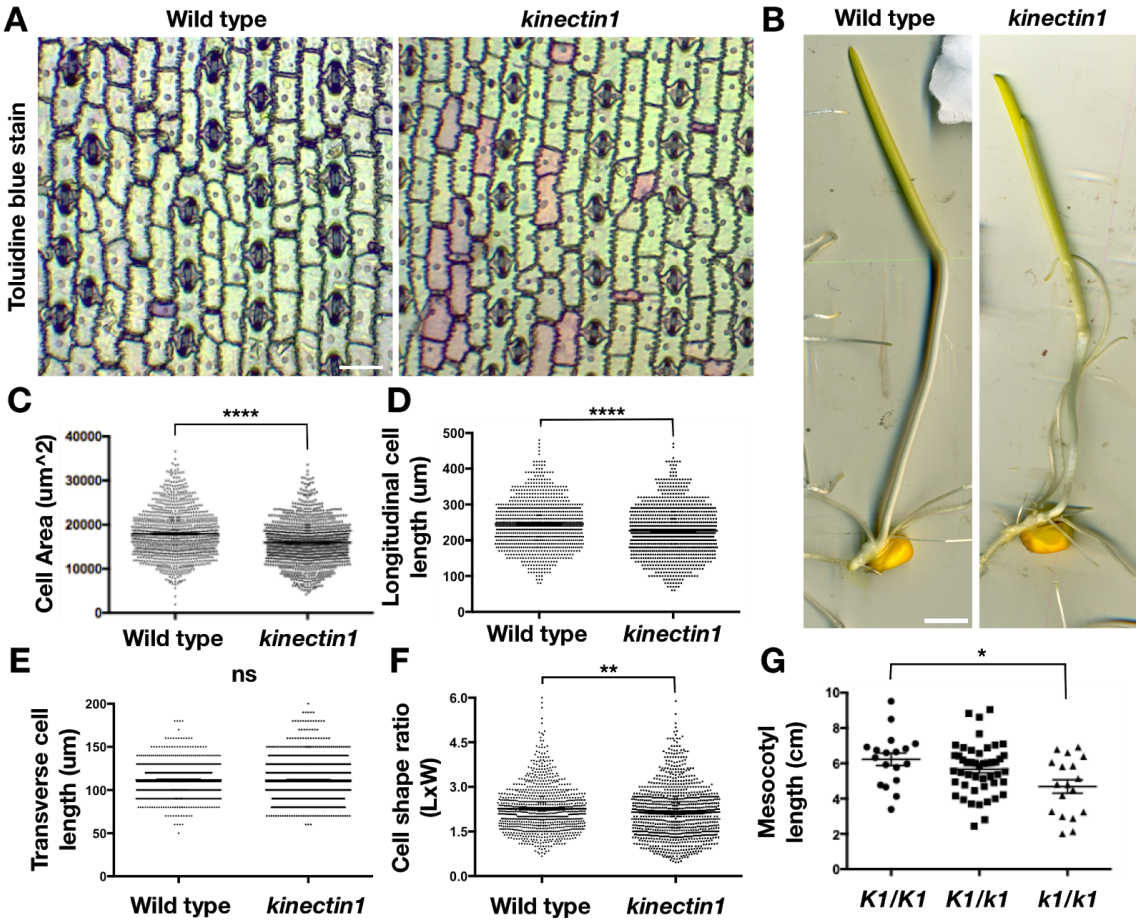
A
Wild type
kinectin1
Toluidine blue stain
B
Wild type
kinectin1
C
Cell Area (um^2)
****
Wild type
kinectin1
D
Longitudinal cell length (um)
****
Wild type
kinectin1
E
Transverse cell length (um)
ns
Wild type
kinectin1
F
Cell shape ratio (LxW)
**
Wild type
kinectin1
G
Mesocotyl length (cm)
*
K1/K1
K1/k1
k1/k1

Figure 3.3: Cell shape and plant growth defects observed in *kinectin* mutants. (A) Micrographs of Toluidine blue O stained maize leaf epidermal peels taken from wild type and *kinectin* mutant plants grown in standard greenhouse conditions. Scale bar is set to 50 μm. Similar results were observed from >100 planes of view from 17 plants. (B) Image of wild type and *kinectin* maize seedling grown in the dark. Similar results were observed from >100 plants. (C) Dot plots of cell areas from maize leaf epidermis pavement cells of wild type and *kinectin* mutant plants. The median area for wild type cells (17,200 +/- 182 μm^2) was calculated using 1,001 cells from 8 plants. The median value for *kinectin* mutant cells (15,600 +/- 160 μm^2) was calculated using 916 cells from 7 plants. The difference in cell area is considered significant using a Mann-Whitney test, $P < 0.0001$. (D) Dot plots of longitudinal cell length from maize leaf pavement cells of wild type and *kinectin* mutant plants. The median length for wild type cells (240 μm +/- 2.3) was calculated using 1,001 cells from 8 plants. The median value for *kinectin* mutant cells (220 μm +/- 2.3) was calculated using 916 cells from 7 plants. The difference in longitudinal cell length is considered significant using a Mann-Whitney test, $P < 0.0001$. (E) Dot plots of transverse cell length from maize leaf epidermis brick cells of wild type and *kinectin* mutant plants. The median length for wild type cells (110 μm +/- 0.61) was calculated using 1,001 cells from 8 plants. The median value for *kinectin* mutant cells (110 μm +/- 0.75) was calculated using 916 cells from 7 plants. (F) Dot plots of cell shape ratios from maize leaf epidermis brick cells of wild type and *kinectin* mutant plants. Values were calculated by dividing the longitudinal cell length by the transverse cell length and quantified as a ratio. The median cell shape ratio for wild type cells (2.2 +/- 0.026) was calculated using 1,001 cells from 8 plants. The median value for *kinectin* mutant cells (2.1 +/- 0.028) was calculated using 916 cells from 7 plants. The difference in longitudinal cell length is considered significant using a Mann-Whitney test, $P = 0.0025$. (G) Dot plots of mesocotyl length from wild-type, heterozygous and homozygous *kinectin* plants grown in the dark. The median mesocotyl length for wild-type plants (6.5 +/- 0.35 cm) was calculated using 18 plants. The median mesocotyl length for heterozygotes (5.9 +/- 0.21 cm) was calculated using 47 plants. The median mesocotyl length for *kinectin* mutants (4.8 +/- 0.38 cm) was calculated using 18 plants. Similar results were observed in three technical replicates with a total of >50 biological replicates of each genotype. The difference in mesocotyl length between wild type and heterozygous plants is not significant. The difference in mesocotyl length between wild type *KINECTIN* and *kinectin* mutant plants is significant using a Mann-Whitney test, $P = 0.0106$. The difference in mesocotyl length between heterozygous and *kinectin* homozygous plants is significant using a Mann-Whitney test, $P = 0.0497$.

KINECTIN is a regulator of microtubule organization and TANGLED1 localization.

Previous reports have shown that KINECTIN localization and function are intimately tied to microtubule-associated proteins in animal cells (Vignal et al. 2001). A split YFP experiment in Arabidopsis protoplasts revealed an interaction between KINECTIN and TUBULIN (Park et al. 2014). Furthermore, cell shape defects that lead to more isotropic cell shapes (Fig 3.2F) are reportedly caused by altered patterns of microtubule organization at the cell cortex (Deng et al. 2015; Kirik et al. 2007; Camilleri et al. 2002).

I used live-cell confocal microscopy to observe cell cortex microtubules in *kinectin* and wild type plants expressing RFP-TUBULIN (Fig 3.3A). Microtubules in the *kinectin* mutants (Fig 3.3E) had a higher median anisotropic pattern of organization during interphase (0.062, n = 344 cells from 3 plants) compared to wild type (0.085, n = 324 cells from 3 plants). However, the orientation (Fig 3.3F) and distribution (Fig 3.3G) of these microtubule arrays was significantly different, with a median angle of 44 degrees in *kinectin* mutant cells and 23 degrees in wild type cells. The growing microtubule plus-end tracking protein EB1-RFP (Chan et al. 2003) was used (Fig 3.3C) to measure microtubule growth dynamics. There was a significant (P = 0.001) increase in the speed of microtubule growth of *kinectin* mutant cells (Fig 3.3H). This data supports the hypothesis that cell shape

defects in the *kinectin* mutant are a direct result of altered microtubule dynamics and improper microtubule organization at the cell cortex during interphase.

In an effort to better understand how KINECTIN impacts microtubule dynamicity and cell cycle progression, I observed expanding phragmoplasts during telophase. The phragmoplast is a highly dynamic structure that guides the cell plate toward the division site during telophase (Smertenko 2018). To promote proper phragmoplast expansion, microtubules are stabilized near the leading edge of the phragmoplast and destabilized near the lagging edge. The median expansion rate was 0.13 um/min at the leading edge and 0.17 um/min at the lagging edge of the phragmoplast in wild type cells. However, the median phragmoplast assembly speed (0.08 μm/min) and disassembly speed (0.09 μm/min) were significantly slower in *kinectin* mutant cells (Fig 3.3I). This data suggests that KINECTIN has a role in microtubule organization during mitosis as well. Further analysis of *kinectin* cells during mitosis may shed light on how microtubule organization defects affect cell cycle progression.

Although division plane positioning was normal in *kinectin* mutant cells, microtubule dynamics and cell shape were not. The microtubule-associated protein TANGLED1 is essential for division plane maintenance and is a microtubule bundling protein (P. Martinez et al. 2019). Using live-cell confocal

microscopy I observed TANGLED1 localization during mitosis in *kinectin* and wild type plants expressing CFP-TUBULIN and TANGLED1-YFP (Fig 3.3J). I found that TANGLED1-YFP localization at the division site was observed in *kinectin* mutant cells. However, the relative fluorescence intensity of TANGLED1 in the spindle was significantly ($P = 0.0125$) increased in *kinectin* cells compared to wild type (Fig 3.3K). This data provides preliminary evidence that KINECTIN protein acts on microtubule-associated proteins in plant cells. Future experiments investigating these relationships further can help to shed light on how microtubule organization becomes altered by KINECTIN in plants.

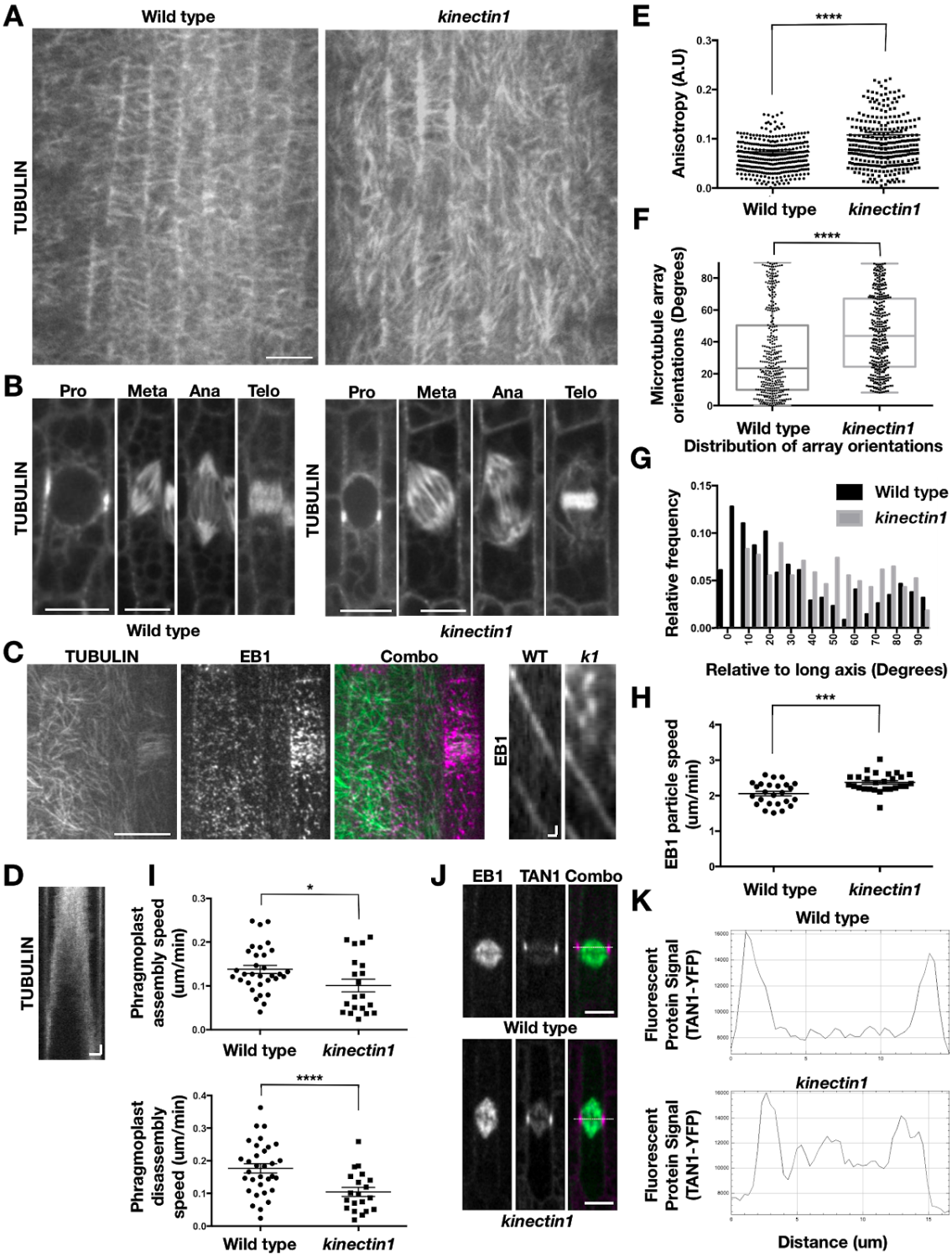
A
Wild type
kinectin1
TUBULIN
B
Pro
Meta
Ana
Telo
TUBULIN
Wild type
kinectin1
C
TUBULIN
EB1
Combo
WT
k1
EB1
D
TUBULIN
E
Anisotropy (A.U)
****
Wild type
kinectin1
F
Microtubule array orientations (Degrees)
****
Wild type
kinectin1
Distribution of array orientations
G
Relative frequency
Wild type
kinectin1
Relative to long axis (Degrees)
H
EB1 particle speed (um/min)
***
Wild type
kinectin1
I
Phragmoplast assembly speed (um/min)
*
Wild type
kinectin1
Phragmoplast disassembly speed (um/min)
****
Wild type
kinectin1
J
EB1
TAN1
Combo
Wild type
kinectin1
K
Wild type
Fluorescent Protein Signal (TAN1-YFP)
kinectin1
Fluorescent Protein Signal (TAN1-YFP)
Distance (um)

Figure 3.4: Microtubule organization, dynamicity and TANGLED1 localization defects observed in *kinectin* mutant cells. (A) Micrograph of cell cortex interphase microtubules in wild type and *kinectin* mutant cells in the dividing zone of the maize leaf epidermis. Scale bar is set to 10 μm. RFP-TUBULIN was used to mark microtubules. (B) Micrographs of mitotic microtubule structures in wild type and *kinectin* mutant maize epidermis cells in the dividing zone of the leaf. Scale bar is set to 10 μm. YFP-TUBULIN was used to mark microtubules. (C) Micrographs of microtubules (left, green) and the growing microtubule plus-end (center, magenta) in wild type maize epidermis cells in the dividing zone of the leaf. Scale bar is set to 10 μm. Kymograph of interphase microtubule growth trajectories from wild type and *kinectin* mutant cells. Horizontal scale bar is set to 1 μm. Vertical scale bar is set to 15 seconds. CFP-TUBULIN was used to mark microtubules. EB1-RFP was used to mark the growing plus-end of microtubules. (D) Kymograph of phragmoplast expansion from a wild type cell. Kymographs of expanding phragmoplasts were obtained using the Multi kymograph function in FIJI, by tracing a line across the primary axis of phragmoplast expansion. Horizontal scale bar is set to 2 μm. Vertical scale bar is set to 1.5 minutes. (E) Dot plots of cell cortex interphase microtubule array anisotropy. The median value for wild type cells (0.062 +/- 0.004 A.U.) was calculated using interphase microtubule arrays at the cell cortex from 344 cells of 6 plants. The median value for *kinectin* mutant cells (0.085 +/- 0.005 A.U.) was calculated using interphase microtubule arrays at the cell cortex from 324 cells of 6 plants. The difference in microtubule array anisotropy is considered significant using a Mann-Whitney test, $P < 0.0001$. (F) Dot plots of cell cortex interphase microtubule array angles from wild type and *kinectin* mutant cells. The median value for wild type cells (23 +/- 1.5 Degrees) was calculated using interphase microtubule arrays at the cell cortex from 344 cells of 6 plants. The median value for *kinectin* cells (44 +/- 1.3 Degrees) was calculated using interphase microtubule arrays at the cell cortex from 324 cells of 6 plants. The difference in microtubule array orientation is considered significant using a Mann-Whitney test, $P < 0.0001$. (G) Bar graph of cell cortex interphase microtubule array angle distributions in wild type and *kinectin* mutant cells. Data was collected from 344 wild type cells (6 plants) and 324 *kinectin* cells (6 plants). The distribution of microtubule array orientations is considered significantly different using an F-test, $P = 0.01$. (H) Dot plots of cell cortex interphase microtubule plus-end growth speed in wild type and *kinectin* mutant cells. The median interphase microtubule growth speed in wild type cells (2.1 +/- 0.06 μm/min) was calculated using 25 microtubules from 7 cells of 3 plants. The median value for *tangled1* mutant cells (2.3 +/- 0.05 μm/min) was calculated using 27 microtubule arrays from 8 cells of 3 plants. The difference in microtubule plus-end growth speed is considered significant using a Mann-Whitney test, $P = 0.001$. (I) Dot plots of phragmoplast assembly and disassembly in wild type and *kinectin* mutant cells during

telophase. Values were calculated by tracing a line over the outer (assembly) and inner (disassembly) edge of the phragmoplast signal in a kymograph and measuring the slope. The median phragmoplast assembly speed (0.13 +/- 0.01 μm/min) and disassembly speed (0.17 +/ 0.01 μm/min) in wild type cells was calculated using 16 phragmoplasts from 3 plants. The median phragmoplast assembly speed (0.08 +/- 0.01 μm/min) and disassembly speed (0.09 +/ 0.01 μm/min) in kinectin mutant cells was calculated using 10 phragmoplasts from 3 plants. The difference in phragmoplast assembly speed between wild type and *kinectin* mutant cells is considered significant using a Mann-Whitney test, P = 0.04. The difference in phragmoplast disassembly speed between wild type and *kinectin* mutant cells is considered significant using a Mann-Whitney test, P = 0.0009. (J) Micrographs of metaphase spindles and TANGLED1 localization from a wild type and *kinectin* mutant cell during mitosis. Microtubules are marked by EB1-RFP (left, green) and TANGLED1 is marked by TANGLED1-YFP (middle, magenta) and images are overlaid in the right panel. Scale bar is set to 10um. Similar results were observed in 33 cells from 6 plants. (K) Relative TANGLED1-YFP fluorescence signal at the division site and metaphase spindle in wild type and *kinectin* mutant cells during mitosis. Fluorescence was measured using the line plot feature in FIJI, by tracing a line across the cell where TANGLED1 signal at the division site was highest. The vertical axis shows fluorescent signal and is measured in arbitrary units. The horizontal axis shows position of signal and is measured in um. The difference in TANGLED1-YFP signal in the metaphase spindle between wild type (median signal of 0.65 +/- 0.03 A.U.) and *kinectin* mutant (median signal of 0.76 +/- 0.03 A.U.) cells is considered significant using a Mann-Whitney test, P = 0.0125. The difference in TANGLED1-YFP signal at the division site is not considered significant using a Mann-Whitney test.

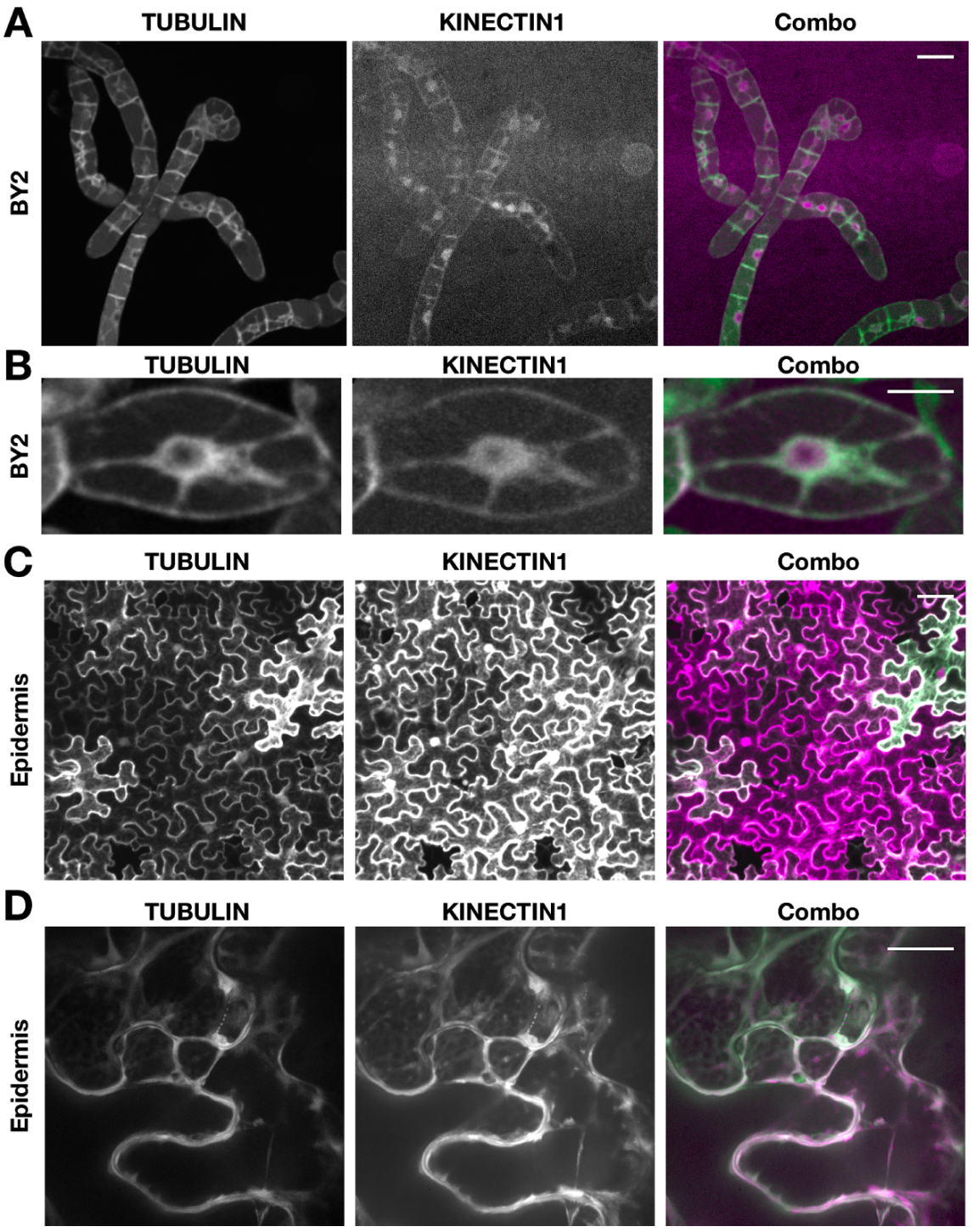
A
TUBULIN
KINECTIN1
Combo
BY2
B
TUBULIN
KINECTIN1
Combo
BY2
C
TUBULIN
KINECTIN1
Combo
Epidermis
D
TUBULIN
KINECTIN1
Combo
Epidermis

Supplemental Figure 3.1 KINECTIN1 localization in Tobacco BY2 and leaf epidermis cells . (A & B) 35S:YFP:*At*KINECTIN1 (magenta) and 35S:RFP:*At*αTUBULIN6 (green) expression in Tobacco BY2 cells during interphase. Scale bar is 100 μm (A) and 20 μm (B). Similar results were observed in >50 cells. (C & D) Transient overexpression with 35S:YFP:*At*KINECTIN1 and 35S:RFP:*At*αTUBULIN6 expression in Tobacco leaf epidermis cells during interphase. Scale bar is 100 μm (C) and 20 μm (D). Similar results were observed in >3 plants.

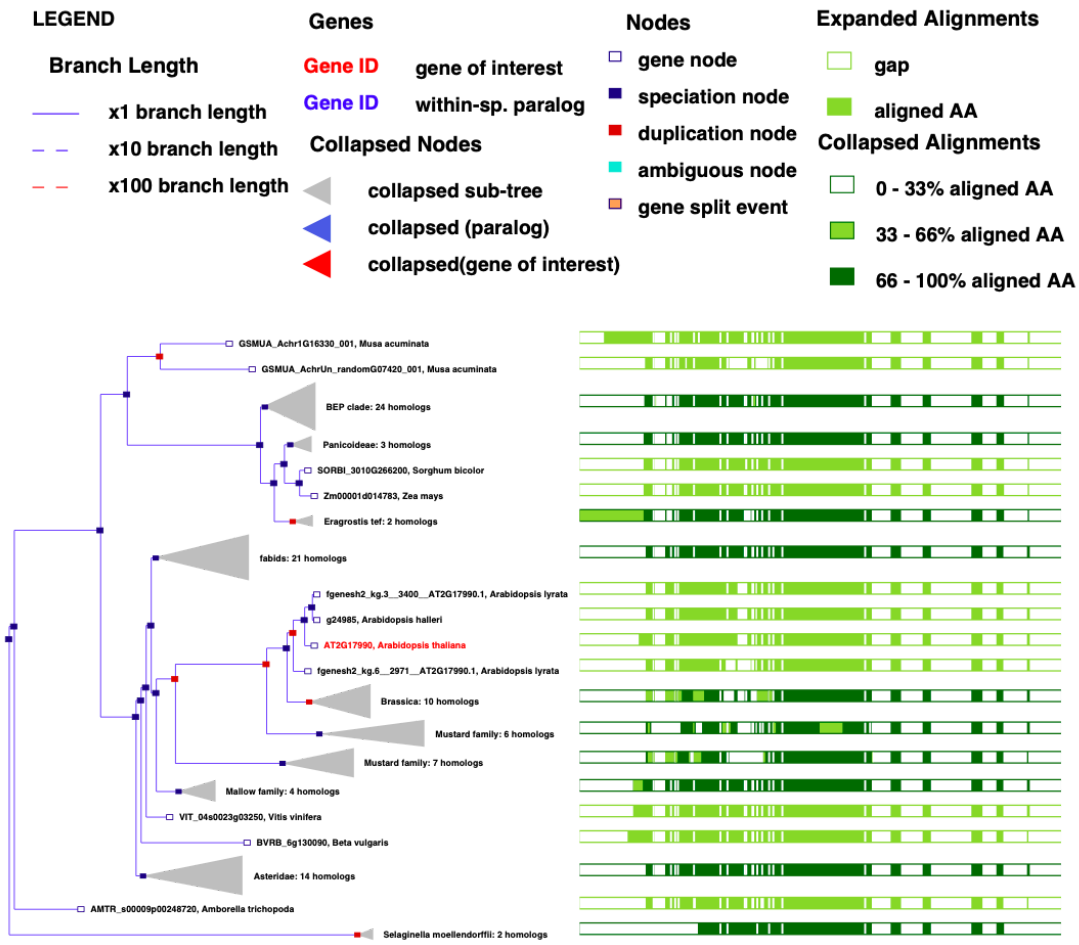

Supplemental Figure 3.2 Phylogenetic analysis and amino acid sequence alignment of KINECTIN in plants. A phylogenetic tree of all currently known KINECTIN-like genes (left) and cartoon diagrams of amino acid sequence conservation among plant KINECTIN proteins (right). This phylogenetic tree and amino acid sequence alignment were done using the gene tree function at ensembl.gramene.org.

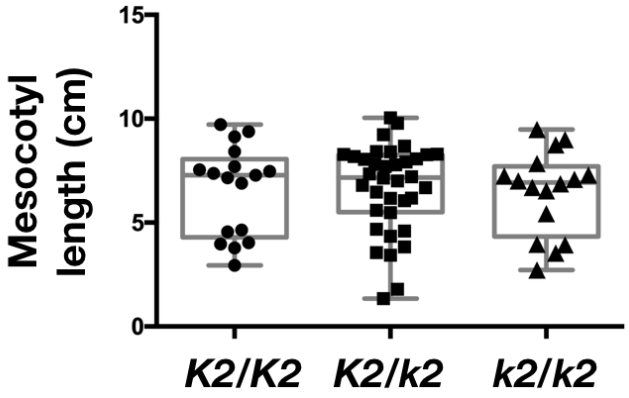

Supplemental Figure 3.3 Dot plots of mesocotyl length from wild-type, heterozygous and homozygous *kinectin-2* plants grown in the dark. The median mesocotyl length for wild-type plants (7.28 cm) was calculated using 17 plants. The median mesocotyl length for heterozygotes (7.17 cm) was calculated using 36 plants. The median mesocotyl length for *kinectin-2* mutants (6.94 cm) was calculated using 18 plants. Similar results were observed in three technical replicates with a total of >50 biological replicates of each genotype. The difference in mesocotyl length between wild type and *kinectin-2* mutants or heterozygous plants is not significant, using a Mann-Whitney test (P = 0.5102 and 0.8282 respectively).

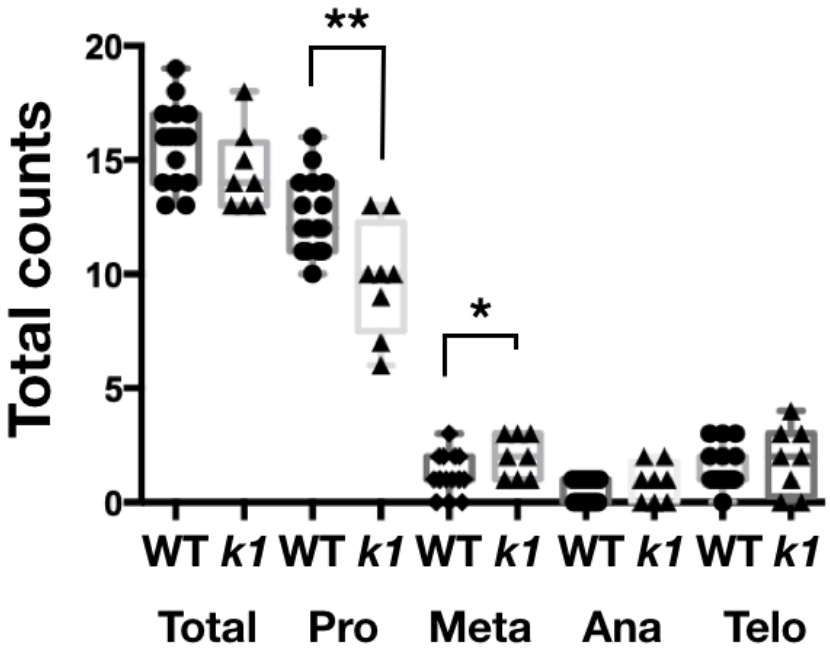

Supplemental Figure 3.4 Dividing cells and mitotic microtubule structures in wild type and *kinectin* mutant plants. Maize leaf epidermis cells were observed at 40x magnification in the dividing region of the leaf during mitosis. Total dividing cells were calculated for each genotype by adding cells in each phase of the cell cycle, preprophase or prophase, metaphase, anaphase and telophase per field of view (n = 8 fields of view from one *kinectin* mutant, n = 16 fields of view from two wild-type plants). The median number of dividing cells per field of view was 16.5 for wild type and 14 for *kinectin* mutants. The difference in dividing cells per field of view is not significant by a Mann-Whiteny U-test. Cells during preprophase or prophase (Pro) were identified by the presence of a preprophase band. The median number of cells with a preprophase band per field of view was 12 for wild type and 10 for *kinectin* mutants. This difference is significant, P = 0.0077. Cells during metaphase (Meta) were identified by the presence of a metaphase spindle. Cells during anaphase (Ana) were identified by the presence of an anaphase spindle. The median number of cells with a spindle per field of view was 1 for wild type and 1 for *kinectin* mutants. This difference is significant, P = 0.0363. Cells during telophase (Telo) were identified by the presence of a phragmoplast. The median number of cells with a phragmoplast per field of view was 1 for wild type and 2 for *kinectin* mutants. This difference is not significant.

DISCUSSION

Microtubule-associated proteins have essential roles in cell shape determination in plants (Krtková, Benáková, and Schwarzerová 2016). To produce specific cell shapes, the proper organization of microtubules is important during division (Cleary and Smith 1998; Camilleri et al. 2002; Schaefer et al. 2017; Komis et al. 2017) and cell expansion (Kirik et al. 2007; Deng et al. 2015; Furutani et al. 2000). In a previous chapter, I showed that TANGLED1 is essential for the proper organization of cell cortex telophase microtubules. In an effort to understand the microtubule independent mechanism for TANGLED1 localization at the division site (Walker et al. 2007), KINECTIN was identified as a direct TANGLED1 interacting protein via a Yeast-2-hybrid screen (Su 2012). KINECTIN has been shown to alter the activity of microtubule-associated proteins by direct binding in animal cells (Ong et al. 2000).

A recent study reported that KINECTIN interacts with TUBULIN in Arabidopsis protoplast cells (Park et al. 2014). My analysis of 90 KINECTIN amino acid sequences from various plant families revealed a conservation of protein-protein interaction domains but not microtubule binding domains (Supplementary Fig 3.2). Additionally, KINECTIN was not reported to colocalize with microtubules in Arabidopsis or *Mesembryanthemum crystallinum* cells (Kwon et al. 2018; Chehab, Patharkar, and Cushman 2007). KINECTIN-YFP localization is likely

cytoplasmic, from live-cell imaging of Arabidopsis leaf and root cells (Fig. 3.2), tobacco epidermis cells (Supplemental 3.1A & B) and BY-2 cells (Supplemental 3.1C & D).

Using *CRISPR*-CAS9, the *KINECTIN* gene region was mutagenized in maize. The *kinectin* mutants had no obvious division plane orientation defects, compared to wild type. However, cells were small and more isotropic. Additionally, mesocotyl length was short in *kinectin-1* maize seedlings grown in the dark, but not *kinectin-2*. The *kinectin-2* allele is predicted to form a functional protein missing the first coiled-coil domain (Fig. 3.1C). These results reveal that KINECTIN has an essential role in cell expansion that requires all three coiled-coil domains in maize.

The phenotypes reported here are common among mutants with microtubule organization defects. Using live-cell imaging, I observed that microtubules were more anisotropically organized at higher angles in *kinectin* mutant cells compared to wild type during interphase. Microtubule growth speed was increased and phragmoplast disassembly speed was reduced in *kinectin* mutants. Finally, TANGLED1 accumulation in the spindle was increased. Together, these results suggest that *kinectin* is essential for proper microtubule organization in plants, likely through regulating microtubule-associated protein

activity. Additional experiments that describe KINECTIN-TUBULIN interaction in vitro and KINECTIN-KINESIN interaction will be required to more clearly demonstrate the latter.

MATERIALS AND METHODS

Plant growth and imaging conditions. Maize plants were grown in 1L pots in standard greenhouse conditions, 16-h light, 8-h dark at University of California, Riverside. Maize plants between 3 and 4 weeks old were imaged. Maize plants segregating YFP-TUBULIN, CFP-TUBULIN, RFP-TUBULIN, TANGLED1-YFP, EB1-mCHERRY or *tangled1* were identified by microscopy or by genotyping. Leaves were removed until the ligule height was <2 mm. Adaxial symmetrically dividing leaf blade samples were mounted in water and covered with Fisherbrand microscope cover glass 24X30-1.5 or loaded into a Rose chamber. Cells were collected from more than 3 plants of each phenotype. The imaging temperature was 23C for images captured on the Zeiss LSM880 and 21C for images captured on the custom-built spinning disk from Solamere Technology (P. Martinez et al. 2017). Arabidopsis plants were grown in sterile conditions on ½ MS plates closed with 3M micropore tape and grown in a chamber at 24C, 16-h light, 8-h dark. Arabidopsis plants between 3 and 5 days post germination were imaged (Gattolin et al. 2009). Arabidopsis plants segregating CFP-TUBULIN, YFP-KINECTIN, KINECTIN-YFP, or *kinectin1* were identified by microscopy or genotyping. Whole

plants were mounted in water on microscope cover glass 24X30-1.5 (Fisher Scientific). Cells were imaged from more than 3 plants. Root epidermal and cortex cells from the meristematic zone were imaged. Images were captured on the Zeiss LSM880 at a temperature of 23C. Tobacco plants were grown with sungro - growing mix soil in 5.5'' pots in a growth room at 24C, 16-h light, 8- dark. Tobacco plants between 2 and 3 weeks old were inoculated by infiltration on the abaxial side of the leaf and imaged 3 days later (Sparkes et al. 2006). Leaf sections were mounted in water on microscope cover glass 24X30-1.5 (Fisher Scientific). Cells were imaged from more than 3 plants. Images were captured on the Zeiss LSM880 at a temperature of 23C. Tobacco BY2 cells were transformed and cultured in liquid BY2 media (MS salts (Murashige and Skoog 1962), Sucrose, Myo-inositol, Thyamine solution, 2,4,D solution and KH_2PO_4) in a shaker at room temperature using a modified protocol from (Brandizzi et al. 2003). Cells were mounted in BY2 media on microscope cover glass 24X30-1.5 (Fisher Scientific). Images were captured on the Zeiss LSM880 at a temperature of 23C.

Adult maize leaf tissue collection and imaging. Maize plants were grown in 2 gallon pots in standard greenhouse conditions, 16-h light, 8-h dark at University of California, Riverside. Leaf 10 of 10 week old adult maize plants were collected. 1cm x 1cm sections were collected from leaves exactly 10 cm above the ligule and fixed as described in (Bellinger, Sidhu, and Rasmussen 2019). Maize leaf

epidermis was peeled and stained with TBO for analysis as described in the same protocol. Values for pavement cell size and dimensions were calculated by first converting the image to black and white and thresholding with the median function in FIJI and analyzed with the Analyze Particles function. Data was exported to google sheets and statistical significance was determined with a Mann-Whitney *U*-test.

Dark grown maize seedling mesocotyl analysis. Kernels were surface sterilized and imbibed with water overnight as described in (J. C. Martinez and Wang 2009). Sterilized kernels were plated on ½MS media (Murashige and Skoog 1962) in magenta boxes, wrapped in foil and grown in a chamber at 24C, 16-h light, 8-h dark for 10 days. Seedlings were removed from magenta boxes and placed on a flatbed scanner. Mesocotyls were measured as described in (Farrow, et al. 2020) and statistical significance was determined with a Mann-Whitney *U*-test.

Confocal microscopy. Fluorescence was recorded using a Zeiss LSM 880 equipped with Airyscan with a 100x, NA = 1.46, oil immersion objective lens Images captured using the Zeiss LSM 880 were processed using Airyscan on default settings with ZEN software (Zeiss). or a custom-built spinning disk from Solamere Technology with a Yokogawa W1 spinning disk, EM-CCD camera from Hamamatsu 9100c and Nikon Eclipse TE inverted stand with a 20x, NA - 0.07, air objective lense; 40x, NA - 1.15, water immersion lens; 60x, NA - 1.2, water

immersion lens; 100x, NA - 1.45, oil immersion objective lens. The stage of the custom-built spinning disk microscope was fully motorized and controlled with Micromanager-1.4 with ASI Peizo, 300um range, and 3 axis DC servo motor controller. The custom-built spinning disk microscope used solid-state lasers from Obis between 40 to 100mW and standard emission filters from Chroma Technology. For YFP-TUBULIN TANGLED1-YFP, YFP-KINECTIN or KINECTIN-YFP a 514 laser with emission filter 540/30 was used. For CFP-TUBULIN a 445 laser with emission filter 480/40 was used. For EB1-mCHERRY or RFP-TUBULIN a 561 laser with emission filter 620/60 was used. Type FF Microscope immersion oil (Cargille was used with 100x objective lenses.)

Images were captured at the cell cortex using adjacent interphase cortical microtubule arrays as a point of reference. Cells during preprophase or prophase were identified by the presence of a preprophase band. Cells during metaphase were identified by the presence of a metaphase spindle. Cells during anaphase were identified by the presence of an anaphase spindle. Cells during telophase were identified by the presence of a phragmoplast. Two-dimensional projections, time projections and three dimensional reconstructions of Z stacks and time-lapse images were generated with Fiji http://rsb.info.nih.gov/ij/. Image color was altered using the linear levels option, color merges and figures were assembled with GIMP-2.10.8 https://www.gimp.org/downloads/. Horizontal drift

was corrected in Fiji with StackReg https://imagej.net/StackReg using the translation option. Photo bleaching was corrected in FIJI using the Simple Ratio method.

Time lapse and quantification of microtubule growth. EB1-mCHERRY was used to label the growing plus-ends of microtubules. A 3 second time interval was used. For analysis of microtubule growth kymographs were created in Fiji as described in (Zanic 2016). Differences in microtubule growth speed was analyzed with PRISM https://www.graphpad.com/ and statistical significance was determined with a Mann-Whitney *U*-test.

Quantification of microtubule array organization. RFP-TUBULIN was used to label the microtubule cytoskeleton. To measure anisotropy, TIFF image files of the cell cortex were converted to PNG files using Fiji software and processed with the FibrilTool plugin (Boudaoud et al. 2014). Differences in anisotropy and were analyzed with PRISM and statistical significance was determined with a Mann-Whitney *U*-test.

Analysis of KINECTIN amino acid and nucleotide sequences. *Homo sapiens* KINECTIN was identified using the NCBI database system (official gene symbol: KTN1, gene_id: 3895) and the amino acid sequence was downloaded and run through the conserved domain database. *Zea mays* KINECTIN was identified using the gramene.org database system (Gene: Zm00001d014783) and the RefGen_v4 amino acid and nucleotide sequence was downloaded. The amino

acid sequence was run through the conserved domain database and compared to the human KINECTIN amino acid sequence results. Human and maize versions of the KINECTIN amino acid sequence were both uploaded to the NCBI database and aligned using the BLASTp suit, Align sequence Protein BLAST tool. The maize KINECTIN nucleotide sequence was uploaded to the A Plasmid Editor software and colored with the Add Feature feature. Cartoon diagrams of gene and protein models were created using Keynote software.

REFERENCES

Ausubel, Frederick M., Roger Brent, Robert E. Kingston, David D. Moore, J. G. Seidman, John A. Smith, and Kevin Struhl, eds. 2001. “CRISPR/Cas9-Based Multiplex Genome Editing in Monocot and Dicot Plants: CRISPR/Cas9-Based Multiplex Genome Editing in Plants.” In *Current Protocols in Molecular Biology*, 8:31.6.1–31.6.21. Hoboken, NJ, USA: John Wiley & Sons, Inc.

Bellinger, Marschal, Sukhmani Sidhu, and Carolyn Rasmussen. 2019. “Staining Maize Epidermal Leaf Peels with Toluidine Blue O.” *BIO-PROTOCOL*. https://doi.org/10.21769/bioprotoc.3214.

Boudaoud, Arezki, Agata Burian, Dorota Borowska-Wykręt, Magalie Uyttewaal, Roman Wrzalik, Dorota Kwiatkowska, and Olivier Hamant. 2014. “FibrilTool, an ImageJ Plug-in to Quantify Fibrillar Structures in Raw Microscopy Images.” *Nature Protocols* 9 (2): 457–63.

Brandizzi, Federica, Sarah Irons, Anne Kearns, and Chris Hawes. 2003. “BY-2 Cells: Culture and Transformation for Live Cell Imaging.” *Current Protocols in Cell Biology / Editorial Board, Juan S. Bonifacino ... [et Al.]* Chapter 1 (August): Unit 1.7.

Buschmann, Henrik, Monika Hauptmann, Dierk Niessing, Clive W. Lloyd, and Anton R. Schäffner. 2009. “Helical Growth of the Arabidopsis Mutant tortifolia2 Does Not Depend on Cell Division Patterns but Involves Handed Twisting of Isolated Cells.” *The Plant Cell* 21 (7): 2090–2106.

Camilleri, Christine, Juliette Azimzadeh, Martine Pastuglia, Catherine Bellini, Olivier Grandjean, and David Bouchez. 2002. “The Arabidopsis TONNEAU2 Gene Encodes a Putative Novel Protein Phosphatase 2A Regulatory Subunit Essential for the Control of the Cortical Cytoskeleton.” *The Plant Cell* 14 (4): 833–45.

Chan, Jordi, Grant M. Calder, John H. Doonan, and Clive W. Lloyd. 2003. “EB1 Reveals Mobile Microtubule Nucleation Sites in Arabidopsis.” *Nature Cell Biology* 5 (11): 967–71.

Chehab, E. Wassim, O. Rahul Patharkar, and John C. Cushman. 2007. “Isolation and Characterization of a Novel v-SNARE Family Protein That Interacts with a Calcium-Dependent Protein Kinase from the Common Ice Plant, Mesembryanthemum Crystallinum.” *Planta* 225 (4): 783–99.

Cleary, A. L., and L. G. Smith. 1998. “The Tangled1 Gene Is Required for Spatial Control of Cytoskeletal Arrays Associated with Cell Division during Maize Leaf Development.” *The Plant Cell* 10 (11): 1875–88.

Deng, Zhu Yun, Ling Tong Liu, Tang Li, Song Yan, Bai Jian Kuang, Shan Jin Huang, Chang Jie Yan, and Tai Wang. 2015. “OsKinesin-13A Is an Active Microtubule Depolymerase Involved in Glume Length Regulation via Affecting Cell Elongation.” *Scientific Reports* 5 (March): 9457.

Furutani, I., Y. Watanabe, R. Prieto, M. Masukawa, K. Suzuki, K. Naoi, S. Thitamadee, T. Shikanai, and T. Hashimoto. 2000. “The SPIRAL Genes Are Required for Directional Control of Cell Elongation in Aarabidopsis Thaliana.” *Development* 127 (20): 4443–53.

Gattolin, Stefano, Mathias Sorieul, Paul R. Hunter, Roman H. Khonsari, and Lorenzo Frigerio. 2009. “In Vivo Imaging of the Tonoplast Intrinsic Protein Family in Arabidopsis Roots.” *BMC Plant Biology* 9 (November): 133.

Horio, Tetsuya, and Takashi Murata. 2014. “The Role of Dynamic Instability in Microtubule Organization.” *Frontiers in Plant Science* 5 (October): 511.

Kirik, Viktor, Ullrich Herrmann, Chaithanyarani Parupalli, John C. Sedbrook, David W. Ehrhardt, and Martin Hülskamp. 2007. “CLASP Localizes in Two Discrete Patterns on Cortical Microtubules and Is Required for Cell Morphogenesis and Cell Division in Arabidopsis.” *Journal of Cell Science* 120 (Pt 24): 4416–25.

Komis, George, Ivan Luptovčiak, Miroslav Ovečka, Despina Samakovli, Olga Šamajová, and Jozef Šamaj. 2017. “Katanin Effects on Dynamics of Cortical Microtubules and Mitotic Arrays in Arabidopsis Thaliana Revealed by Advanced Live-Cell Imaging.” *Frontiers in Plant Science* 8 (May): 866.

Krtková, Jana, Martina Benáková, and Kateřina Schwarzerová. 2016. “Multifunctional Microtubule-Associated Proteins in Plants.” *Frontiers in Plant Science* 7 (April): 474.

Kumar, J., H. Yu, and M. P. Sheetz. 1995. “Kinectin, an Essential Anchor for Kinesin-Driven Vesicle Motility.” *Science* 267 (5205): 1834–37.

Kwon, Yun, Jinbo Shen, Myoung Hui Lee, Kyoung Rok Geem, Liwen Jiang, and Inhwan Hwang. 2018. “AtCAP2 Is Crucial for Lytic Vacuole Biogenesis during Germination by Positively Regulating Vacuolar Protein Trafficking.” *Proceedings of the National Academy of Sciences of the United States of America* 115 (7): E1675–83.

Lee, Peter L., Maikke B. Ohlson, and Suzanne R. Pfeffer. 2015. “Rab6 Regulation of the Kinesin Family KIF1C Motor Domain Contributes to Golgi Tethering.” *eLife* 4 (March). https://doi.org/10.7554/eLife.06029.

Lin, Shaoyu, Sha Sun, and Junjie Hu. 2012. “Molecular Basis for Sculpting the Endoplasmic Reticulum Membrane.” *The International Journal of Biochemistry & Cell Biology* 44 (9): 1436–43.

Martinez, J. C., and K. Wang. 2009. “A Sterilization Protocol for Field-Harvested Maize Mature Seed Used for in Vitro Culture and Genetic Transformation.” *Maize Genetics Cooperation Newsletter* 83. http://agron-www.agron.iastate.edu/ptf/publications/Martinez_MGCNL_2009.pdf.

Martinez, Pablo, Ram Dixit, Rachappa S. Balkunde, Seán E. O’Leary, Kenneth A. Brakke, and Carolyn G. Rasmussen. 2019. “TANGLED1 Mediates Interactions between Microtubules That May Promote Spindle Organization and Phragmoplast Guidance to the Division Site in Maize.” *bioRxiv*. https://doi.org/10.1101/711796.

Martinez, Pablo, Anding Luo, Anne Sylvester, and Carolyn G. Rasmussen. 2017. “Proper Division Plane Orientation and Mitotic Progression Together Allow Normal Growth of Maize.” *Proceedings of the National Academy of Sciences of the United States of America* 114 (10): 2759–64.

Murashige, Toshio, and Folke Skoog. 1962. “A Revised Medium for Rapid Growth and Bio Assays with Tobacco Tissue Cultures.” *Physiologia Plantarum* 15 (3): 473–97.

Nakamura, Masayoshi, David W. Ehrhardt, and Takashi Hashimoto. 2010. “Microtubule and Katanin-Dependent Dynamics of Microtubule Nucleation Complexes in the Acentrosomal Arabidopsis Cortical Array.” *Nature Cell Biology* 12 (11): 1064–70.

Ong, L. L., A. P. Lim, C. P. Er, S. A. Kuznetsov, and H. Yu. 2000. “Kinectin-Kinesin Binding Domains and Their Effects on Organelle Motility.” *The Journal of Biological Chemistry* 275 (42): 32854–60.

Paredez, Alexander R., Christopher R. Somerville, and David W. Ehrhardt. 2006. “Visualization of Cellulose Synthase Demonstrates Functional Association with Microtubules.” *Science* 312 (5779): 1491–95.

Park, Guen Tae, Jennifer M. Frost, Jin-Sup Park, Tae Ho Kim, Jong Seob Lee, Sung Aeong Oh, David Twell, Janie Sue Brooks, Robert L. Fischer, and Yeonhee Choi. 2014. “Nucleoporin MOS7/Nup88 Is Required for Mitosis in Gametogenesis and Seed Development in Arabidopsis.” *Proceedings of the National Academy of Sciences of the United States of America* 111 (51): 18393–98.

Rasmussen, Carolyn G., Brian Sun, and Laurie G. Smith. 2011. “Tangled Localization at the Cortical Division Site of Plant Cells Occurs by Several Mechanisms.” *Journal of Cell Science* 124 (Pt 2): 270–79.

Sapala, Aleksandra, Adam Runions, Anne-Lise Routier-Kierzkowska, Mainak Das Gupta, Lilan Hong, Hugo Hofhuis, Stéphane Verger, et al. 2018. “Why Plants Make Puzzle Cells, and How Their Shape Emerges.” *eLife* 7 (February). https://doi.org/10.7554/eLife.32794.

Schaefer, Estelle, Katia Belcram, Magalie Uyttewaal, Yann Duroc, Magali Goussot, David Legland, Elise Laruelle, Marie-Ludivine de Tauzia-Moreau, Martine Pastuglia, and David Bouchez. 2017. “The Preprophase Band of Microtubules Controls the Robustness of Division Orientation in Plants.” *Science* 356 (6334): 186–89.

Schopfer, Peter, Catherine Lapierre, and Titus Nolte. 2001. “Light-Controlled Growth of the Maize Seedling Mesocotyl: Mechanical Cell-Wall Changes in the Elongation Zone and Related Changes in Lignification.” *Physiologia Plantarum* 111 (1): 83–92.

Smertenko, Andrei. 2018. “Phragmoplast Expansion: The Four-Stroke Engine That Powers Plant Cytokinesis.” *Current Opinion in Plant Biology* 46 (December): 130–37.

Smith, L. G., S. M. Gerttula, S. Han, and J. Levy. 2001. “Tangled1: A Microtubule Binding Protein Required for the Spatial Control of Cytokinesis in Maize.” *The Journal of Cell Biology* 152 (1): 231–36.

Smith, L. G., S. Hake, and A. W. Sylvester. 1996. “The Tangled-1 Mutation Alters Cell Division Orientations throughout Maize Leaf Development without Altering Leaf Shape.” *Development* 122 (2): 481–89.

Sparkes, Imogen A., John Runions, Anne Kearns, and Chris Hawes. 2006. “Rapid, Transient Expression of Fluorescent Fusion Proteins in Tobacco Plants and Generation of Stably Transformed Plants.” *Nature Protocols* 1 (4): 2019–25.

Su, Tianying. 2012. “Proteins That Interact with Arabidopsis TANGLED.” https://escholarship.org/uc/item/5bx9v4v9.pdf.

Toyoshima, I., H. Yu, E. R. Steuer, and M. P. Sheetz. 1992. “Kinectin, a Major Kinesin-Binding Protein on ER.” *The Journal of Cell Biology* 118 (5): 1121–31.

Vignal, E., A. Blangy, M. Martin, C. Gauthier-Rouvière, and P. Fort. 2001. “Kinectin Is a Key Effector of RhoG Microtubule-Dependent Cellular Activity.” *Molecular and Cellular Biology* 21 (23): 8022–34.

Walker, Keely L., Sabine Müller, Dorianne Moss, David W. Ehrhardt, and Laurie G. Smith. 2007. “Arabidopsis TANGLED Identifies the Division Plane throughout Mitosis and Cytokinesis.” *Current Biology: CB* 17 (21): 1827–36.

Zanic, Marija. 2016. “Measuring the Effects of Microtubule-Associated Proteins on Microtubule Dynamics In Vitro.” *Methods in Molecular Biology* 1413: 47–61.

CHAPTER FOUR: Discussion and Future Directions

The work presented here primarily used in-vivo techniques and live-cell imaging to understand how microtubule organization at the cell cortex regulates cell shape in plants. I used a combination of maize leaf, tobacco leaf, Arabidopsis leaf and root epidermis as well as tobacco BY2 cells to describe my findings and make predictions about how microtubule organization at the cell cortex is achieved by TANGLED1 and KINECTIN in plants. To more completely understand how these proteins regulate cell shape via microtubule organization it will be necessary to observe patterns of localization and protein-protein interactions in other plant systems as well. We are only beginning to understand the relationship between KINECTIN and microtubules or microtubule associated proteins in plants. Future in vivo and vitro experiments can help to shed light on how microtubule dynamics are altered by this protein.

The role of the preprophase band and division plane maintenance

TANGLED1 and other proteins with roles in division plane maintenance colocalize with the preprophase band but remain at the cell cortex following preprophase band disassembly (Rasmussen and Bellinger 2018). Genetic mutants with preprophase band assembly defects often express pleiotropic plant growth and microtubule organization defects that can make it difficult to elucidate the functions of proteins with specific roles in division plane positioning (Spinner

et al. 2013). Nevertheless, TANGLED1, POK1, POK2, RANGAP1 and potentially other proteins with roles in division plane maintenance require the preprophase band in order to localize to the division site prior to spindle assembly (Walker et al. 2007; Rasmussen, Sun, and Smith 2011; Xu et al. 2008; Schaefer et al. 2017).

A recent study of an Arabidopsis triple mutant has helped to shed light on the role of the preprophase band in division plane maintenance (Schaefer et al. 2017). It was described here that the *trm678* mutant does not assemble the microtubule component of the preprophase band but expresses normal interphase cortical microtubule array organization compared to wild type. Although POK1 was reported to accumulate at the division site in *trm678* triple mutants, the pattern of localization within the cell was different compared to wild type. These mutants expressed mild division plane maintenance defects.

In *Physcomitrella patens* (moss), gametophore cell division progresses normally in the absence of a preprophase band (Kosetsu et al. 2017). It is currently unknown how or when division site localized proteins like TANGLED1 accumulate at the cell cortex in these cells. Here, spindle orientation plays a central role in division plane positioning in gametophore cells. The over accumulation of TANGLED1 in the metaphase spindles of *kinectin* cells (Fig. 3.4

J & K) could suggest that the TANGLED1-KINECTIN interaction is important for division plane maintenance in plant cells that lack preprophase bands. Using tools to disrupt the *KINECTIN* gene in gametophores, like *CRISPR*/CAS9 or RNA interference may shed light on the role of this protein in microtubule organization and cell shape determination in the absence of the preprophase band. Indeed, the proper organization of microtubules associated with the spindle is essential for proper chromosome segregation as well as division plane maintenance in cell divisions in plants (Yoneda et al. 2005) and animals (Yamashita, Jones, and Fuller 2003; Laan et al. 2012). In yeast, it was shown that the KINESIN proteins KIF1 and KIF3 are both required for proper cell cycle progression and spindle disassembly at the midplane (Ibarlucea-Benitez et al. 2018).

Understanding the role of KINECTIN during mitosis.

The KINESIN family of motor proteins is expanded in plants (>60 in land plants) compared to animals (45 in humans). Specifically, there are a greater number of minus-end directed (KINESIN-14 subfamily) KINESIN proteins in plants (Jonsson et al. 2015; Gicking et al. 2018; Li, Xu, and Chong 2012). Two KINESIN proteins, POK1 and POK2, are important for division plane positioning (Müller, Han, and Smith 2006; Stöckle et al. 2016) and TANGLED1 maintenance at the division site (Walker et al. 2007). KINECTIN has been described as a regulator of KINESIN activity in animal cells (Ong et al. 2000). I have shown that KINECTIN is an

important factor for proper microtubule organization at the cell cortex and phragmoplast expansion.

The endogenous localisome of 43 KINESIN proteins has been described in *Physcomitrella patens (Miki et al. 2014)*. Plus-end and minus-end directed KINESIN proteins have been shown to occupy the same location within microtubules structures, like the interphase cortical microtubule array or phragmoplast. This system may also provide an excellent resource to understand how *kinectin* loss of function mutants impact KINESIN protein localization or activity in plants, which remains an unanswered question.

Although adult *kinectin* mutants had cell shape defects, we did not observe obvious plant growth defects in plants grown in normal greenhouse conditions. Preliminary evidence suggests that *kinectin* mutants may have more cells per field of view compared to wild type. To investigate potential defects in cell cycle progression of *kinectin* mutant cells, I used live-cell confocal microscopy to observe mitotic microtubule structures via CFP labelled TUBULIN (Supplemental Fig. 3.4). The total number of dividing cells was the same between genotypes. However, *kinectin* mutant plants had significantly fewer preprophase bands (10 per field of view, n = 8) and more spindles (1 per field of view, n = 16). This data suggests that *kinectin* mutant cells may move slower through metaphase but faster through preprophase and prophase. The preprophase band, which

assembles before mitosis, lasts ~16 hours, compared to < 1-2 hours for metaphase and telophase (Gunning and Sammut 1990). Future in depth analysis of microtubule structures, together with time-lapse imaging, may shed light on how *kinectin*-associated microtubule organization defects impact cell cycle progression in plants.

REFERENCES

Gicking, Allison M., Kyle W. Swentowsky, R. Kelly Dawe, and Weihong Qiu. 2018. "Functional Diversification of the Kinesin-14 Family in Land Plants." *FEBS Letters* 592 (12): 1918–28.

Gunning, Bes, and M. Sammut. 1990. "Rearrangements of Microtubules Involved in Establishing Cell Division Planes Start Immediately after DNA Synthesis and Are Completed Just before Mitosis." *The Plant Cell* 2 (12): 1273–82.

Ibarlucea-Benitez, Itziar, Luke S. Ferro, David G. Drubin, and Georjana Barnes. 2018. "Kinesins Relocalize the Chromosomal Passenger Complex to the Midzone for Spindle Disassembly." *The Journal of Cell Biology* 217 (5): 1687–1700.

Jonsson, Erik, Moé Yamada, Ronald D. Vale, and Gohta Goshima. 2015. "Clustering of a Kinesin-14 Motor Enables Processive Retrograde Microtubule-Based Transport in Plants." *Nature Plants* 1 (7). https://doi.org/10.1038/NPLANTS.2015.87.

Kosetsu, Ken, Takashi Murata, Moé Yamada, Momoko Nishina, Joanna Boruc, Mitsuyasu Hasebe, Daniël Van Damme, and Gohta Goshima. 2017. "Cytoplasmic MTOCs Control Spindle Orientation for Asymmetric Cell Division in Plants." *Proceedings of the National Academy of Sciences of the United States of America* 114 (42): E8847–54.

Laan, Liedewij, Nenad Pavin, Julien Husson, Guillaume Romet-Lemonne, Martijn van Duijn, Magdalena Preciado López, Ronald D. Vale, Frank Jülicher, Samara L. Reck-Peterson, and Marileen Dogterom. 2012. "Cortical Dynein Controls Microtubule Dynamics to Generate Pulling Forces That Position Microtubule Asters." *Cell* 148 (3): 502–14.

Li, Juan, Yunyuan Xu, and Kang Chong. 2012. "The Novel Functions of Kinesin Motor Proteins in Plants." *Protoplasma* 249 Suppl 2 (June): S95–100.

Miki, Tomohiro, Haruko Naito, Momoko Nishina, and Gohta Goshima. 2014. "Endogenous Localizome Identifies 43 Mitotic Kinesins in a Plant Cell." *Proceedings of the National Academy of Sciences of the United States of America* 111 (11): E1053–61.

Müller, Sabine, Shengcheng Han, and Laurie G. Smith. 2006. "Two Kinesins Are Involved in the Spatial Control of Cytokinesis in Arabidopsis Thaliana." *Current Biology: CB* 16 (9): 888–94.

Ong, L. L., A. P. Lim, C. P. Er, S. A. Kuznetsov, and H. Yu. 2000. “Kinectin-Kinesin Binding Domains and Their Effects on Organelle Motility.” *The Journal of Biological Chemistry* 275 (42): 32854–60.

Rasmussen, Carolyn G., and Marschal Bellinger. 2018. “An Overview of Plant Division-Plane Orientation.” *The New Phytologist*, April. https://doi.org/10.1111/nph.15183.

Rasmussen, Carolyn G., Brian Sun, and Laurie G. Smith. 2011. “Tangled Localization at the Cortical Division Site of Plant Cells Occurs by Several Mechanisms.” *Journal of Cell Science* 124 (Pt 2): 270–79.

Schaefer, Estelle, Katia Belcram, Magalie Uyttewaal, Yann Duroc, Magali Goussot, David Legland, Elise Laruelle, Marie-Ludivine de Tauzia-Moreau, Martine Pastuglia, and David Bouchez. 2017. “The Preprophase Band of Microtubules Controls the Robustness of Division Orientation in Plants.” *Science* 356 (6334): 186–89.

Spinner, Lara, Astrid Gadeyne, Katia Belcram, Magali Goussot, Michaël Moison, Yann Duroc, Dominique Eeckhout, et al. 2013. “A Protein Phosphatase 2A Complex Spatially Controls Plant Cell Division.” *Nature Communications* 4: 1863.

Stöckle, Dorothee, Arvid Herrmann, Elisabeth Lipka, Theresa Lauster, Richard Gavidia, Steffi Zimmermann, and Sabine Müller. 2016. “Putative RopGAPs Impact Division Plane Selection and Interact with Kinesin-12 POK1.” *Nature Plants* 2 (August): 16120.

Walker, Keely L., Sabine Müller, Dorianne Moss, David W. Ehrhardt, and Laurie G. Smith. 2007. “Arabidopsis TANGLED Identifies the Division Plane throughout Mitosis and Cytokinesis.” *Current Biology: CB* 17 (21): 1827–36.

Xu, Xianfeng Morgan, Qiao Zhao, Thushani Rodrigo-Peiris, Jelena Brkljacic, Chao Sylvia He, Sabine Müller, and Iris Meier. 2008. “RanGAP1 Is a Continuous Marker of the Arabidopsis Cell Division Plane.” *Proceedings of the National Academy of Sciences of the United States of America* 105 (47): 18637–42.

Yamashita, Yukiko M., D. Leanne Jones, and Margaret T. Fuller. 2003. “Orientation of Asymmetric Stem Cell Division by the APC Tumor Suppressor and Centrosome.” *Science* 301 (5639): 1547–50.

Yoneda, Arata, Minori Akatsuka, Hidemasa Hoshino, Fumi Kumagai, and Seiichiro Hasezawa. 2005. “Decision of Spindle Poles and Division Plane by Double Preprophase Bands in a BY-2 Cell Line Expressing GFP-Tubulin.” *Plant & Cell Physiology* 46 (3): 531–38.